THE PROPOSED ALIGNMENT SYSTEM FOR THE FINAL FOCUS TEST BEAM AT SLAC*

R. E. RULAND, G. E. FISCHER

Stanford Linear Accelerator Center
Stanford University, Stanford, CA 94309 USA

1. ABSTRACT

This report describes the current state of work in progress with respect to the geometry, alignment requirements, scenarios, and hardware for meeting the tolerances of the Final Focus Test Beam (FFTB) at SLAC. The methods and systems proposed acknowledge that component motion at the micron level, from whatever cause (ground motion, thermal effects, etc.) must be measured on-line and compensated for on relatively short time scales. To provide an integrated alignment/positioning package, some unique designs for reference systems, calibration of effective electric and magnetic centers, and component movers are introduced.

2. INTRODUCTION

The FFTB at SLAC is an experiment, manned by an international collaboration,[1] designed to test advanced linear collider concepts and equipment. The purpose of the work is to focus a 50 GeV electron beam, having uncoupled SLC like emittances[2] down to aberration limited spot sizes of

$$\sigma_y, \sigma_x \approx 60 \text{ nanometers, } 1 \text{ micrometer} .$$

The physical arrangement of optical elements in this beam line is about 300 meters long and requires transverse placement of focusing elements to tolerances that are unattainable by current conventional alignment practices. As shown in Figure 1, about two-thirds of the line is inside a deep underground structure; the remainder in a newly constructed concrete housing which is exposed to the weather. In the following we describe the problem, our present conceptual solutions, and some hardware and environmental tests prior to construction of the system.

*Work supported by Department of Energy contract DE-AC03-76SF00515.

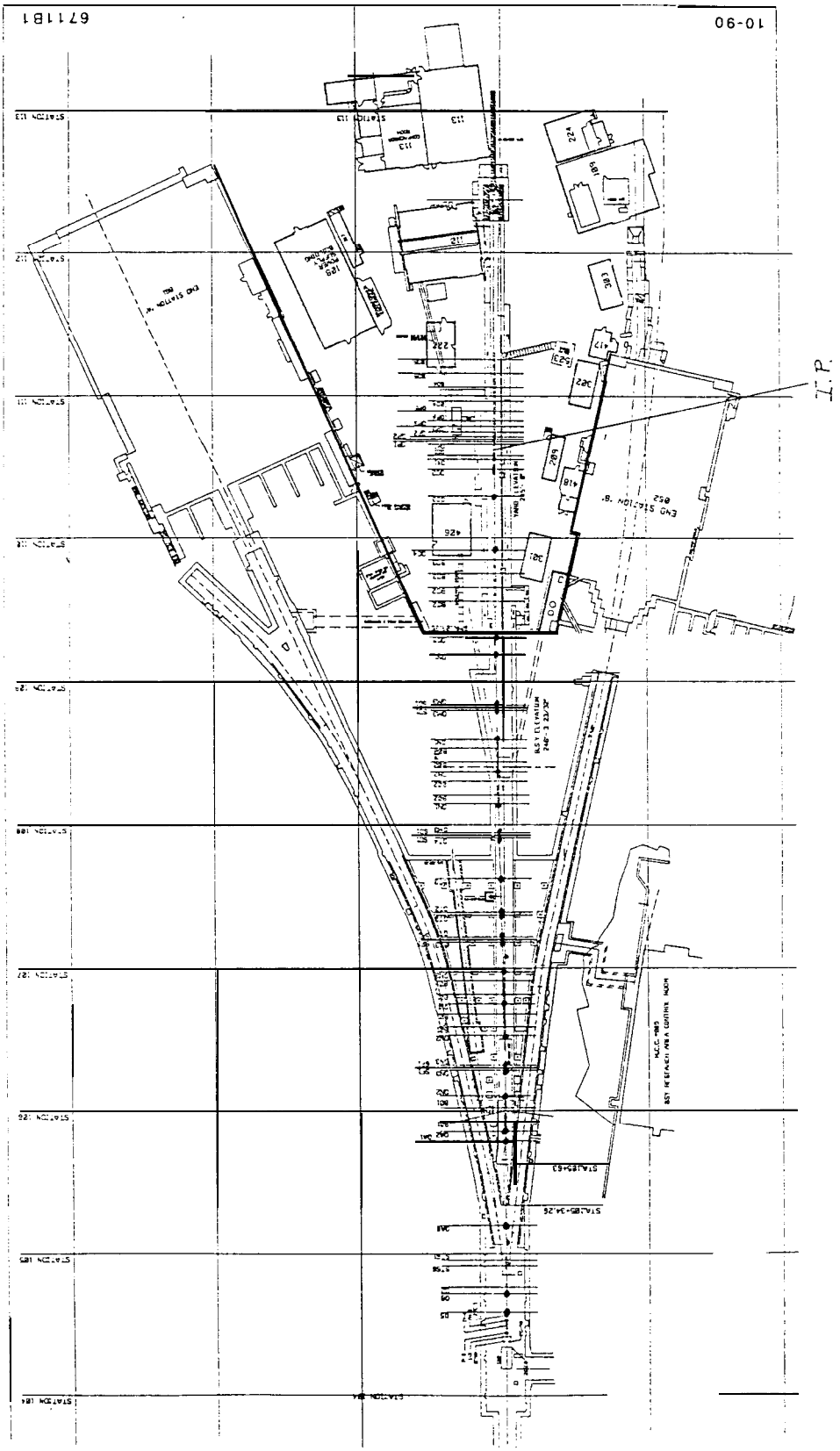

Figure 1 Layout of the Final Focus Test Beam (FFTB) in the central Beam Switchyard and research yard areas of SLAC.

3. ALIGNMENT TOLERANCES

3.1. HISTORICAL BACKGROUND

Over about a year ago, based on early work by J. Murray and K. Oide, we rather arbitrarily set transverse "survey and alignment" tolerances at between 5 to 10 microns.[3] By the summer of 1989, Oide pointed out that the optics were still correctable if the "ab initio" tolerances were as large as 30 microns.[4] To meet absolute tolerances in this range, an on-line alignment system-based on an extended Beam Switchyard laser system–had been proposed in which every quadrupole was referenced to its own laser target station. Although the image sizes of these targets remain diffraction limited, the required resolution could be achieved because target positions enjoy an extreme sensitivity resulting from very large geometric lever arms when they are viewed 3 km away. Since only one target could be inserted at any given time, reading 30 stations would take, perhaps, as long as 30 minutes. This was considered to be too long[5] because it was pointed out that the final focus *interaction point* was located outside the underground tunnel, and would therefore be subjected to ambient temperature changes. Since no one could construct a believable ground motion model of the research yard base, experimental investigations were begun which subsequently indicated rates of motion as high as one micron/minute.[6]

This high rate occurs when the sun rises and heats the volume between End Station A and End Station B. It was proposed that local quadrupole positions be monitored by means of *stretched wires.* Since this technique is most effective for straight lines and limited to lengths of about 50 meters before the wires sag too much, new questions were posed to the opticians; namely: What are the initial and operational alignment tolerances on just those optical elements along the five separate straight line segments of the FFTB?

3.2. NEW ALIGNMENT TOLERANCES[7]

Consider the FFTB to be made up of five (5) hinged straight lines, as layed out in Figure 2(a).

For this discussion, consider four (4) time scales:

1. The period of initial alignment (absolute).
2. The period of initial beam turn-on. "Steering, but without making use of beam spot size measurements." We presume this to mean running quadrupole strengths up and down and observing whether or not the beam moves at the next downstream beam position monitor (which may or may not be on the exact magnetic center of an element). In this manner, the beam is steered to the final spot.
3. Tune the beam by adjusting quadrupole positions and strengths, using spot size measurements. Iterate. Assume a *tuning time* of, say, one hour.
4. Long Term: Stability of motion of elements after returning to the experiment after an interruption of say 24 hours or longer.

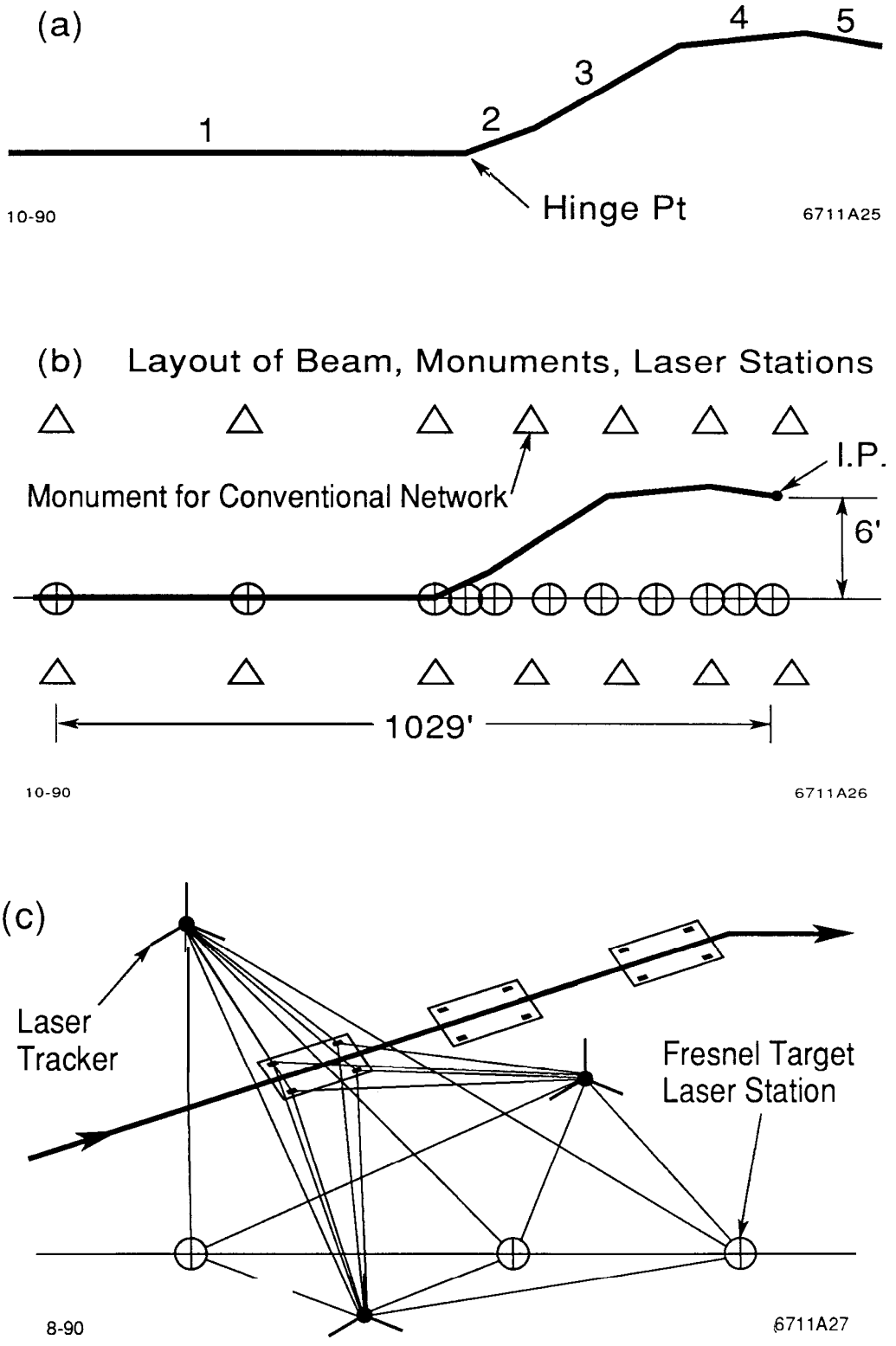

Figure 2. Equivalent Final Focus Test Beam geometry in terms of straight line segments.

Specifications for Period 1: *ab inito* ***alignment w.r.t.*** *design configuration:* The magnetic centers (nodal points) of quadrupoles and sextupoles shall lie within:

$$\delta x_{\text{rms}} < 100\ \mu\text{m} \quad \text{and} \quad \delta y_{\text{rms}} < 30\ \mu\text{m}$$

of each fitted *straight line.* This line intersects the adjacent straight lines at so-called hinge points. Intersection must take place with a distance of closest approach no greater than 30 μm.

The hinge points themselves may deviate from the design trajectory by as much as:

$$\Delta x \approx 2\ \text{mm} \quad \text{and} \quad \text{Ay} \approx 0.2\ \text{mm}\ .$$

Bending magnet power supplies will be adjusted to compensate for the change in geometric angles.

Specifications for Periods 2,3: during tuning: It is expected that lens positions should be *readable and setable* during the tuning procedure with *resolutions* of a *few microns* in general. There are a few lenses (notably QN2) that will require closer attention in position (0.3 μm) and roll ($\theta_z < 10^{-4}$). Roll tolerances are generally of order one milliradian. Pitch and yaw remain to be calculated, but are considered to be loose.

Period 4: long-term reproducibility w.r.t. an absolute fresnel laser system: One would like to have the beam tuning experiments teach the experimenter how to reduce the above tuning times by making use of other intelligence-perhaps predict the behavior of the system if *known* displacements, relative to an absolute reference, can be measured. To this end, one would like (no hard fixed rules can be expected here at this time) to have a *reproducibility* specification read: *measure with respect to an absolute reference system to within*

$$r_x < 15\ \mu\text{m} \quad \text{and} \quad r_y < 5\ \mu\text{m}\ .$$

In addition to the above requests, with respect to *static alignment,* there are operational specifications on jitter (namely motion that is uncorrectable by means of ordinary mechanical magnet movers; i.e., in the range of .001 to 1 Hz). Since spot density dilution (by a factor of two) occurs generally for motions of order 1 μm, such uncorrelated motion should be kept below this value. Higher frequency disturbances not amenable to correction by electrical feedback should be kept below about one spot size at the final focus; i.e., say 60 to 100 nm.

Special requirements on roll (the final lenses and QN2 are examples) should be controllable by means of electrically adjustable skew quadrupoles.

4. THE PRESENT ALIGNMENT PROPOSAL IN TERMS OF A STEP-BY-STEP SCENARIO

4.1. DESCRIPTION

In this section we present a time sequenced approach to achieving the initial placement tolerances for components and their subsequent maintenance (i.e., periods 1 through 4 listed above). This approach recognizes the fact that, for radiation shielding considerations during the construction period, it will not be possible to bring a laser alignment path through the iron muon shielding block in the Beam Switchyard (BSY) and out onto the research yard pad before all construction str activities are complete.

Step 1: Extend a conventional network of temporary monuments through the downstream part of the BSY and out onto the research yard pad. Locations are indicated on the layout (Figure 2b) by the symbol Δ. Since neither the emerging electron beam direction nor the path of the BSY laser light axis is in a horizontal plane (they dip about 5 mrad), it is important at the outset to establish the "s" or "z" coordinates to better than 0.2 mm over the 300-meter length of the system. To accomplish this task, a modern Mekometer[8] is the instrument of choice.

Step 2: Install one laser fresnel target station opposite each *hinge point* and in between hinge points as shown by the symbol $\oplus$. The horizontal and vertical centerlines of these stations are to be as close to the existing and extended laser axis as possible with this conventional technique. Each of these stations has reference tooling outside its vacuum enclosure, as described previously,[9] and is equipped with fine adjustment screws that allow final positioning when the laser system is evacuated and activated.

Step 3: In a similar way, install all beam line components on their Anocast© supports and magnet mover bases to within about one millimeter, using the conventional network laser stations for reference.

Step 4: ***(fiesnel Laser Light System not yet available)*** Use a laser tracker[10]– ~~which~~ is an instrument that combines a theodolite angle measuring system ($\delta\theta \approx$ 2 arcseconds) with an interferometer-retroreflector ranging system-to measure, compute position, fit straightness, and correct location of all elements along each straight segment as shown in the layout by dotted lines (Figure 2c). After several iterations with this technique, which has a resolution of 5 to 10 μm, integrating measurements from several setups using the *Bundle* technique, the straightness of the five fitted segments should be easily within the required 30 μm in the vertical and 100 μm in the horizontal.

If the initial network is good enough and stable enough in defining an absolute reference, then the ends of the segments would be within specification. Were it not for daily ground motions and thermal deformations, the laser light system would not be necessary at all. However, we believe the conventional network will not be good enough and we cannot meet the specification at this step.

If the Fresnel Laser Light System is available at this step, the laser light stations are then aligned along the projected linac accelerator axis to within microns, and provide an absolute and verifiable moment-to-moment reference axis for the laser tracker work described above. Starting from far-better determined locations should considerably shorten the number of iterations required to place components. It should be remembered that the fitting has to be done in three dimensions.

Step 5: Install and activate the on-line straightness monitoring system–"The Wires." In order to achieve the straightness repeatability requirement, each line segment is provided with two fine stretched wires by which the x, y positions (and possibly roll and pitch) of each quadrupole or quadrupole-sextupole-quadrupole package is continuously monitored. See Figure 3(a) for a layout of the wires. Since we do not yet have much operational experience with this concept, it has not yet been decided whether or not the sensors that monitor the transverse coordinates of a component will read absolute or only relative positions in each segment. Readout resolution should be of order 1 to 2 microns in x and y over a range comparable to that of the magnet movers; i.e., 1 to 2 mm. It is hoped the clear aperture of the monitor is in the range 1 to 2 cm to facilitate installation and maintenance of the wires over their 50 meter length.

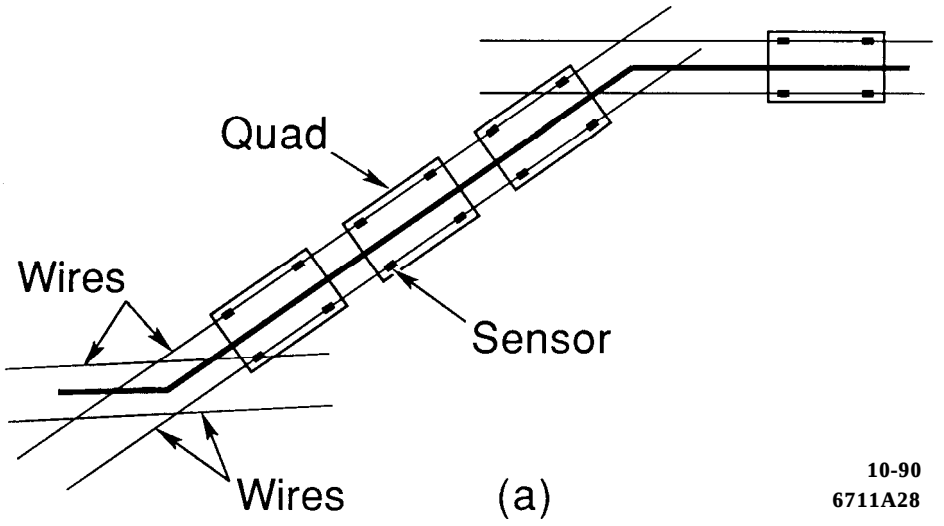

Figure 3(a). Plan view and cross section of stretched-wire straightness system.

Step 6: Install the bridges. The wires serve only to monitor the straightness of the segments, since their ends are fastened more or less arbitrarily. To monitor the ends of the wires relative to the absolute laser axis, bridges are installed as shown on Figure 3(b) which carry the instrumentation to transfer coordinates. Mercury levels having micron resolution and proximity sensors, as suggested in last year's draft proposal, are to be employed for vertical transfer. The extensometer is used

in the horizontal. Absolute horizontal calibrations could be readily performed with the laser tracker. The laser station midway between wire endpoints is provided to ensure the integrity of vertical readout in the event the wires suffer from thermal or other fatigue (quantify the catenary) as well as to provide better spacing in the laser tracker network.

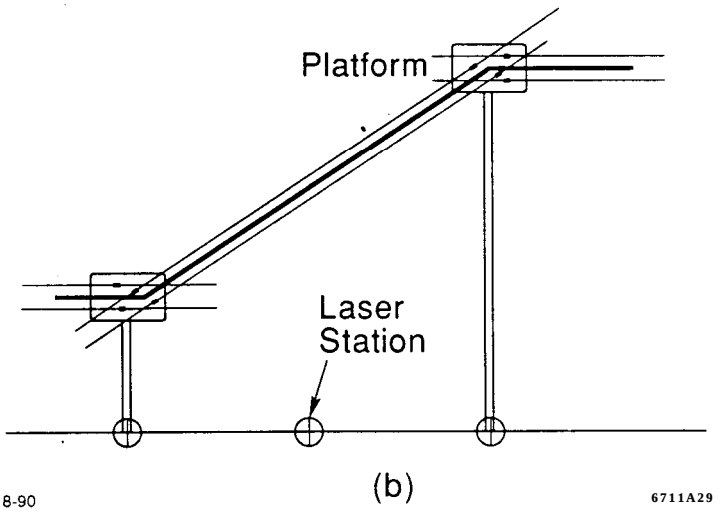

Figure 3(b). Plan view and cross section of stretched-wire straightness system.

Step 7: All parts of the FFTB including the shielding are now in place, and the plugs in the iron wall may be removed, permitting the laser alignment system to be activated. Now the final alignment can begin, as indicated in the latter part of step 4.

4.2. An Appraisal

The reader will note that in this, the current proposal, less emphasis is placed on an absolute reference system to locate and monitor the position of components, and more emphasis is placed on relative locations. This is the result of having noted that the effects of *long-range correlated* errors are never as severe as sharp local errors. Some features of the absolute system are kept, however, to ensure that each time the system is brought up, the tuning procedures should not have to "start from scratch". The practical consequences of the current approach are to dramatically lower the number (hence cost) of laser stations required, and to embark on the development of a wire system with capabilities at the micron level. The existence of instruments like the laser tracker is essential to carrying out this proposal. If it appears that there are too many checks built into this proposal, it is well to recall an important principle in surveying, namely: To *use a given measurement only once in the analysis.* Further, we believe it is one of the functions of this experiment to evaluate which is the most efficient way to solve the problems of the micron world, in which it is not known *a priori* what (the floor, the mounts, the components, or the instrumentation) will be moving.

5. DETAILS OF THE HARDWARE

5.1. THE MAGNET REFERENCE TOOLING FRAME

The effective electromagnetic center of a focusing element or of a beam position monitor, being along the beam path, is not a physical location that can be touched with alignment tools. Some form of practical reference tooling has to be provided. Traditionally, this has been in the form of tooling balls mounted in some convenient place on the object, with the traditional confusion of just where these balls are relative to where the beam thinks the center of the object is. Moreover, thermal expansion of the object changes the location of these tooling balls. The frame, shown sketched in Figure 4, overcomes some of these problems. The legs are brought to bear on the split planes of the magnet which, being symmetry planes, should not change their location with expansion. The legs are made of invar or other material of very low expansion coefficient. The procedure by which this fixture is calibrated is detailed in Section 7.7.

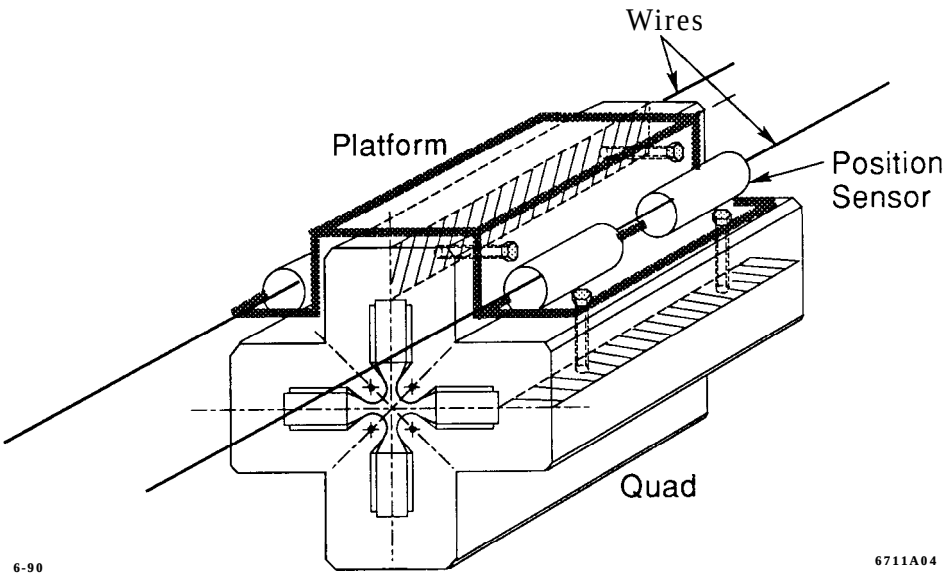

Figure 4. Artists conception of the magnet reference tooling frame.

5.2. THE WIRES[11]

Stretched wires have been used since Egyptian times in aligning large structures[12]. Development of high-precision wires for this application has been taken on by the DESY laboratory.[13]

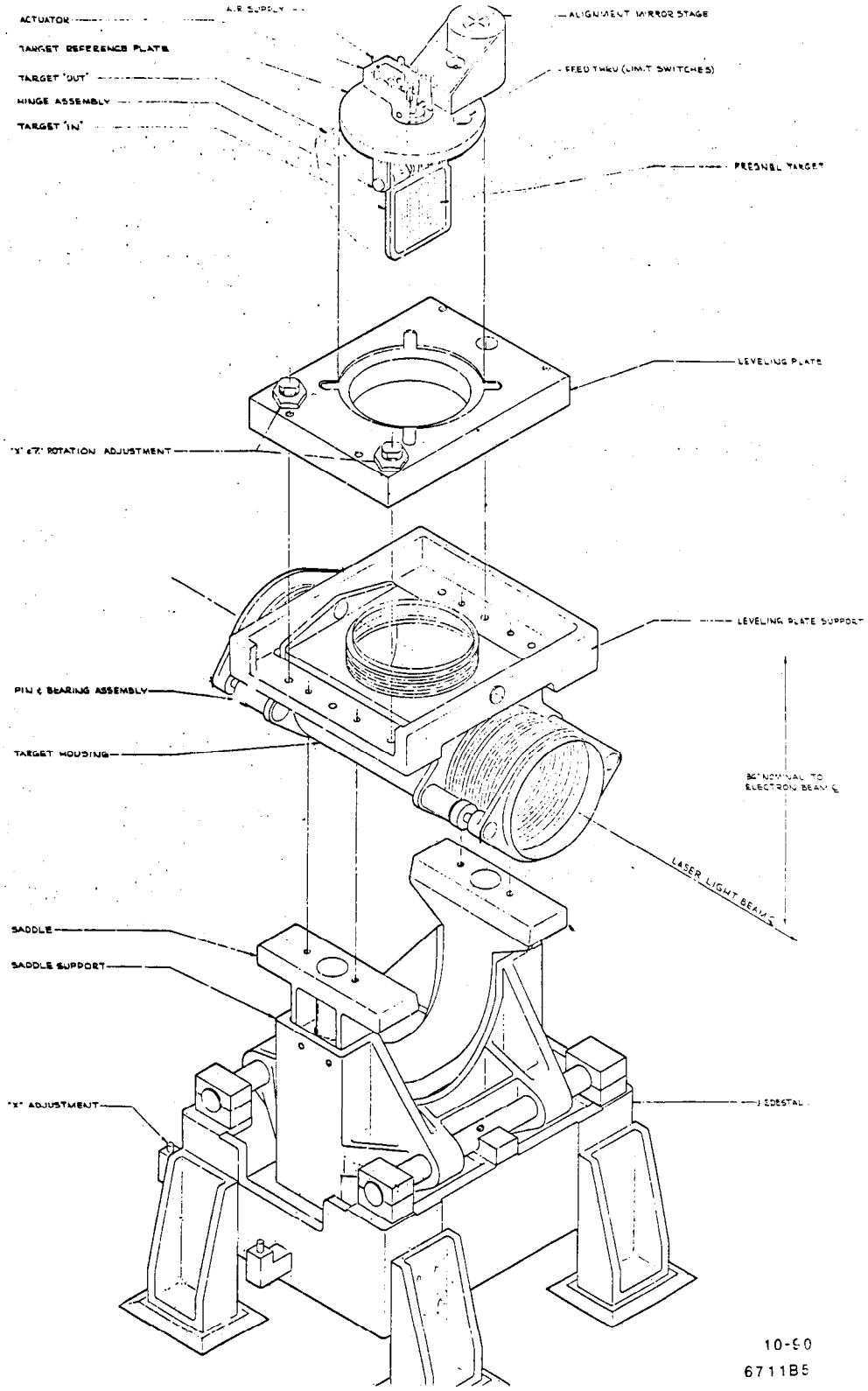

Figure 5. Exploded view of a Beam Switchyard laser station.

5.3. The Fresnel Target Laser System

Description: The existing BSY laser system, its resolution, upgrades, and proposed operation, was described in some detail in the previous *Draft* proposal[14] and the references therein. In this current proposal, the number of laser stations is reduced from twenty-nine (29) to nine (9) new locations. Figure 5 is an exploded view of an existing laser station, showing its saddle, vacuum housing, leveling plate, and actuator assembly. The laser itself, and its mount, will be mounted in the research yard outside the new housing so that, in contrast to its previous location, it can be manipulated during beam operation. We intend to maintain the existing geometry in which the light enters the housing at right angles to the linac axis. We note that since this location is likely to move about during operation, we will employ readings from so-called *stable points* in the BSY and the far end of the linac to define the linac axis.

Recent Experiences with the Beam Switchyard Alignment Laser: On April 25, 1990, it was possible to reactivate the original BSY laser system, and to take data with it, as well as with the main linac laser alignment system. The positions of images were marked on a ground-glass screen, rather than with the usual trolley,

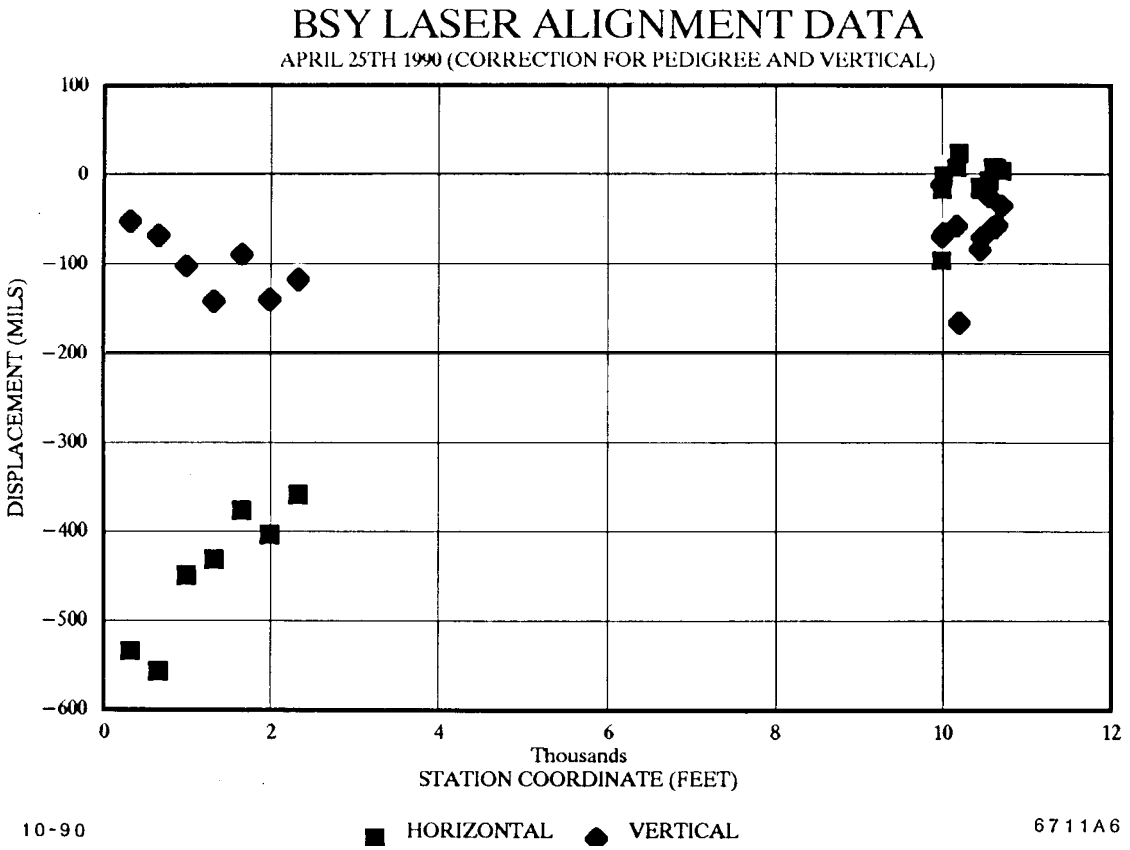

Figure 6. Relative alignment of laser stations in the Beam Switchyard (last moved in 1966).

because they were much displaced with respect to preliminary observations taken in February 1989. Figure 6 shows the analysed data (corrected for station pedigree only in the linac, and referring to a straight line with the laser itself at one end and the center of the glass port in the detector room at the other end).

Figure 7 displays a magnified view of the switchyard data. Ignoring the points from the monument (which was never used for BSY alignment) and station 11 (which was moved during SLC construction), the horizontal readings average to -1 mils and have an rms spread of 10 mils. The vertical readings cluster around -57 mils and have a spread of 17 mils. Our recollection from February 1989 is that the vertical data was tighter then, but it should be mentioned that the new data was not only post-earthquake, but also after many tons of iron shielding were rearranged in the switchyard. These results are very encouraging with respect to the stability of the old BSY tunnel floor.

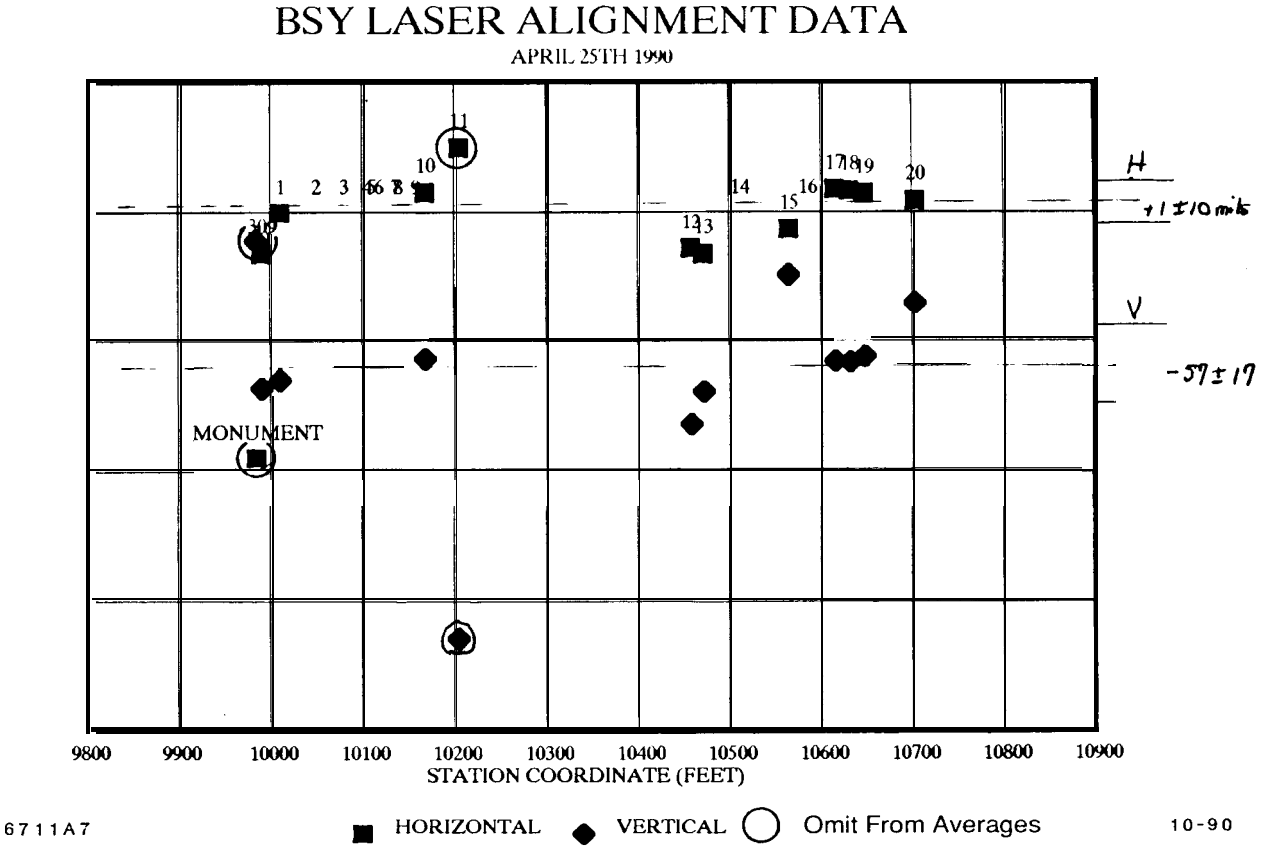

Figure 7. Magnified view of laser lens positions in the Beam Switchyard.

5.4. THE BRIDGE

General: The purpose of the *bridge* is to reference the ends of the wires to the absolute coordinates of the laser stations. A cross section depicting this function is shown in Figure 8. Since the coordinates of these locations are vastly different in both x and y, it is important to maintain the local coordinate frame plumb. Other parts of the bridge include the extensometer, mercury height transfer liquid levels, and tiltmeters.

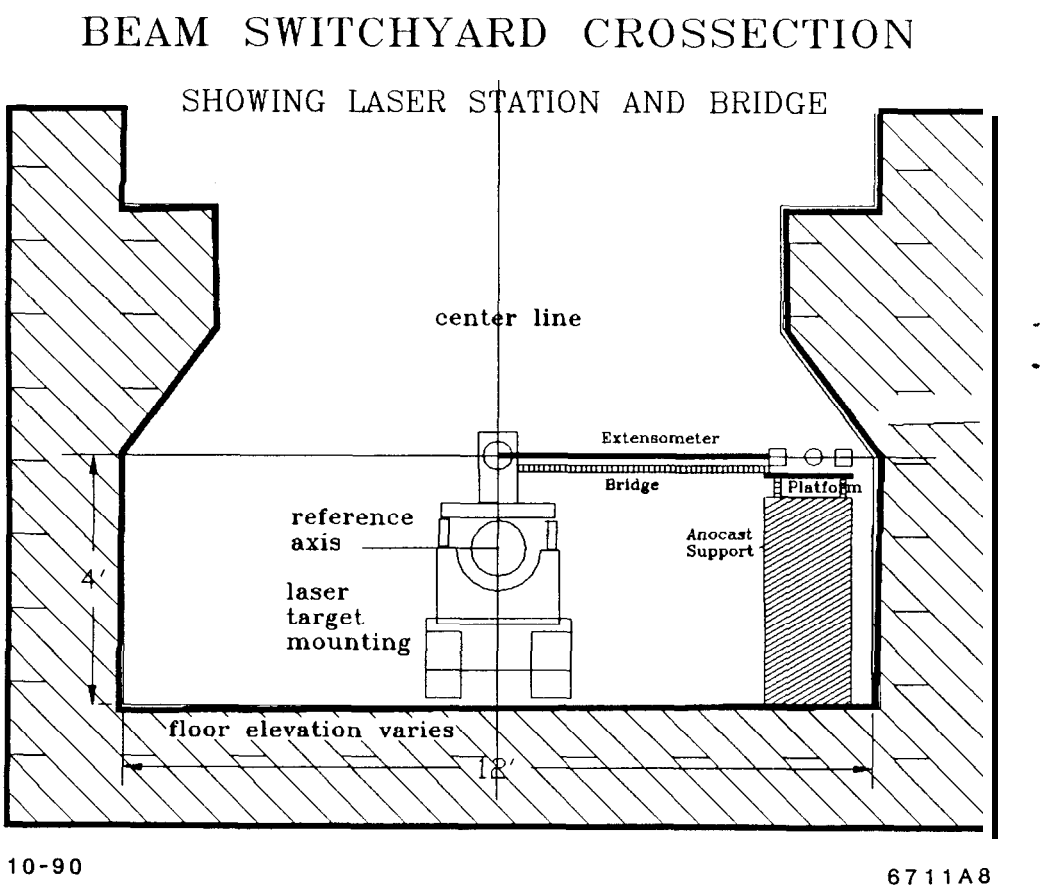

Figure 8. The Coordinate Transfer Bridge (view along the beam direction).

Recent experiences with a precision mercury level: For the past year we have been attempting to develop a precision mercury level to measure height differences in the micron range. The principle requirements on the device are that it provide reproducible results over long periods without drift, and be reasonably radiation hard. When it was pointed out to us that oxygen (a constituent of air) attacks the mercury surface, thereby altering surface tension and hence changing the meniscus-determined height of the liquid, we returned to an all metal (stainless steel) system that can be evacuated and backfilled with dry nitrogen. Various height sensors were examined. The one used in the current version is a capacitance sensor[15] which is housed outside the cell volume and which measures the liquid level by sensing through a thin plastic window (polycarbonate). The assembly is shown

in Figure 9. For these tests, the usable range had been set to ±0.5 mm per cell. The height of the mercury pool is 12 mm. No attempt has yet been made to compensate for height changes due to cell temperature variations. These are expected to be 0.5 microns/ºC. The free period of the instrument is expected to be about 120 seconds.

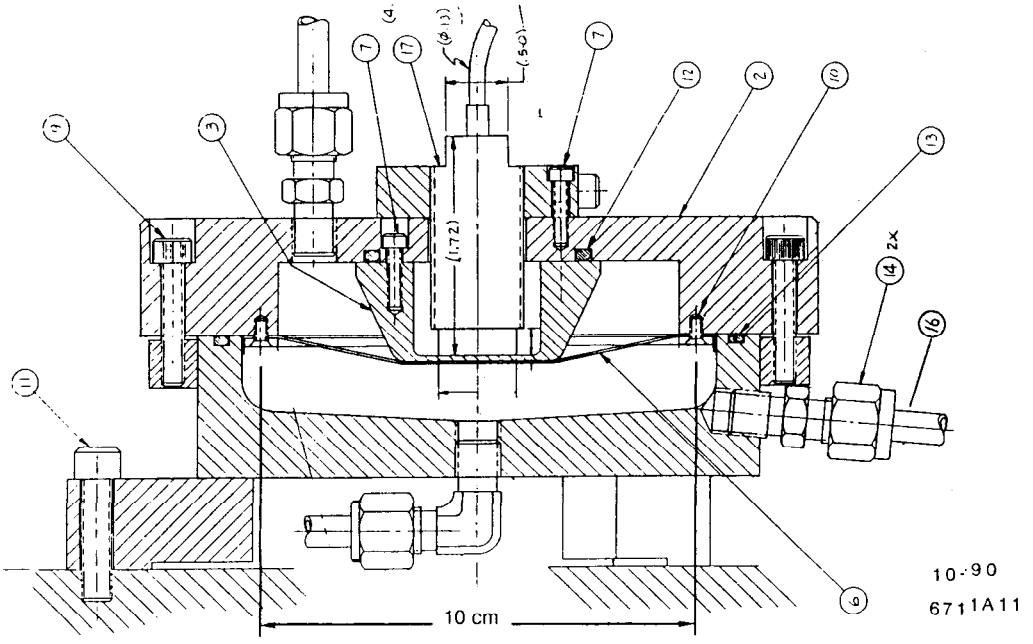

Figure 9. Assembly of precision mercury level cell.

A one-week portion of a two-month trial of two cells (connected two meters apart) resting on the concrete floor of the Central Laboratory Annex basement are shown in Figure 10. Data was logged every ten minutes. A tilt of one microradian represents one cell rising, the other falling by 1 *m*m. The data shown in this figure was taken after covering the cells with thermal insulation, and shows that after several days the cell temperature stabilized at the ground temperature. The other temperature trace represents the air temperature in the room near its east wall. A check made with the aid of a third sensor measuring a fixed distance showed that the signal processing electronics was insensitive to ambient changes, varying no more than one digitizer count for the ambient changes observed. One digitizer count is 179 microvolts, and represents an 18 nanometer liquid height difference.

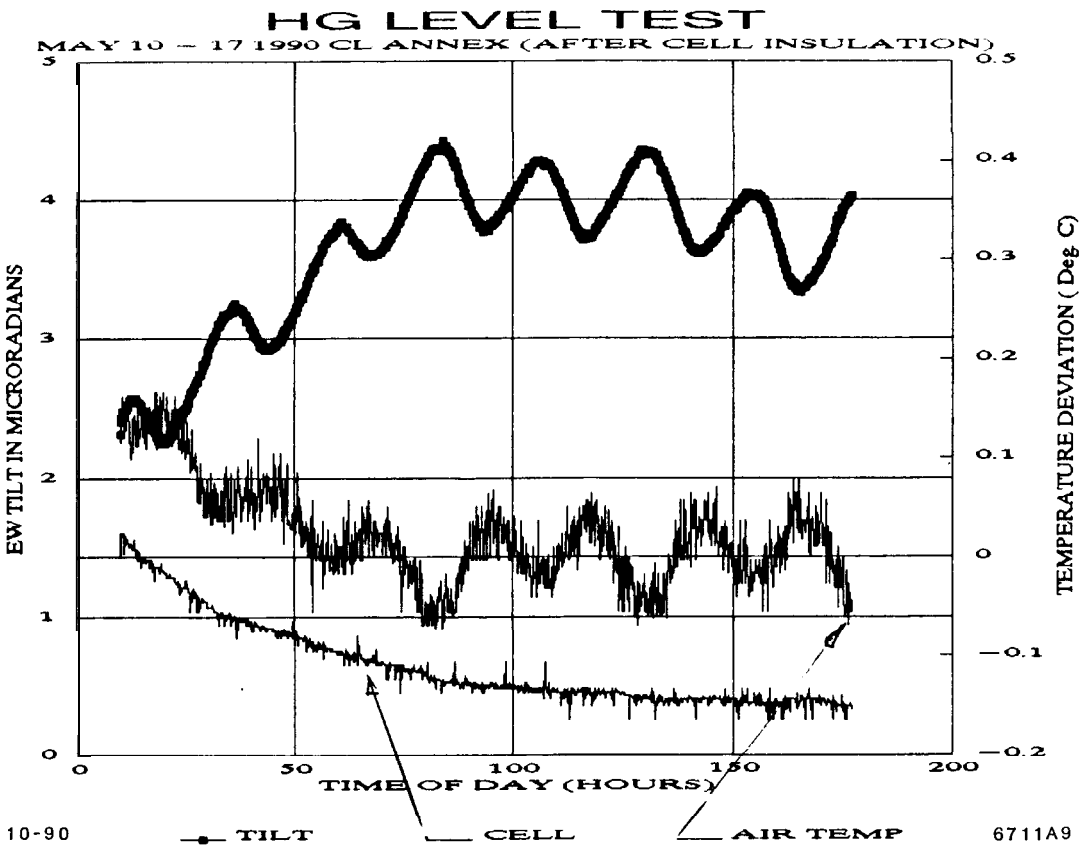

Figure 10. Stability test results from the mercury cell level.

Our current interpretation of the data is as follows. Since ambient temperature changes of the instrument cannot explain the apparent tilt of the floor, we will assume that it is real. The measured period of the oscillation is much closer to 24 hours than 24.8 hours (the period of the moon), and we therefore ascribe the motion to thermal effects outside the experiment, rather than to the earth tides. The ambient air temperature in the room follows the temperature outside of the building. We therefore speculate that the sun heats the east wall of the building preferentially, and thereby tilts the basement floor. (The south wall of the basement is underground.) One notices that the swings of temperature and motion are smaller on cooler days that have overcast skies. Recent tests conducted at the Sector 10 test bench show similar daily fluctuation in tilt (see Figure 11).

We are encouraged, and work of this kind continues on, for example: smaller, more practical, cells; differential eddy current sensors[16] other liquids for the level; and temperature compensated mountings.

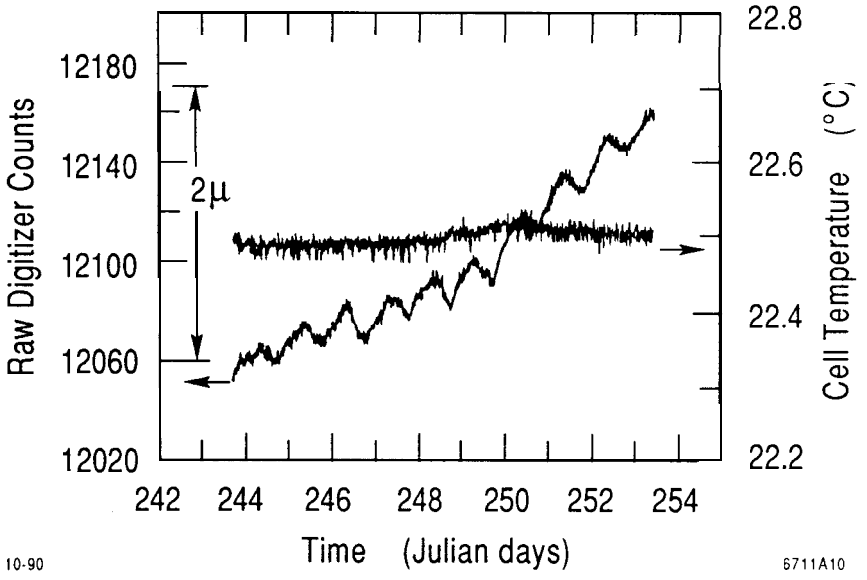

Figure 11. Sector 10 tilt stability results.

5.5. AUXILIARIES

The Inclinometers and Rotation Tables: Using a high-resolution tilt sensor mounted on a rotation table, it is possible to compute the absolute, gravity-relative tilt of a platform or tooling frame upon which wire position monitors and/or proximity sensors are mounted. The FFTB alignment system will use wire position monitors and proximity gauges to track motions of the magnetic centers of focusing magnets at the micron level, with respect to an absolute reference frame. The tracking measurements are performed at some distance, tens of centimeters, from the points being tracked. Assuming that the distance between the points being tracked and measurement devices is constant or can be computed, one must nevertheless know the angular orientation between the measurement devices and the points being tracked. The inclinometer system provides this information. The rotation tables allow to balance systematic errors (bias, zero offset).

The planned resolution of the sensors is one arcsecond (4.85 microradians).

5.6. CONTROLS

The style and architecture of the controls system is constrained by the fact that FFTB operation is part of a much larger accelerator system, namely the SLC, whose controls are CAMAC based and VAX driven. The very complexity of SLC also imposes certain uniformity standards on hardware, and particularly software issues. In order to be operationally *compatible* with SLC the designs of magnet controllers, beam position and profile monitors, magnet mover controls, and the like, are carried over directly to the new system; their overhead has already been accounted for. Less clear have been the issues connected with devices that have no clear precedence, such as the readout of the laser alignment system images, wire position monitors, proximity sensors tiltmeters, and the like. The first cut[17] on their *integration* is shown in Figures 12(a)-(d). Those systems requiring local processing are provided with micros that then communicate with the VAX, employing standard protocol.

(3) Proximity Sensor (Control System Schematic)

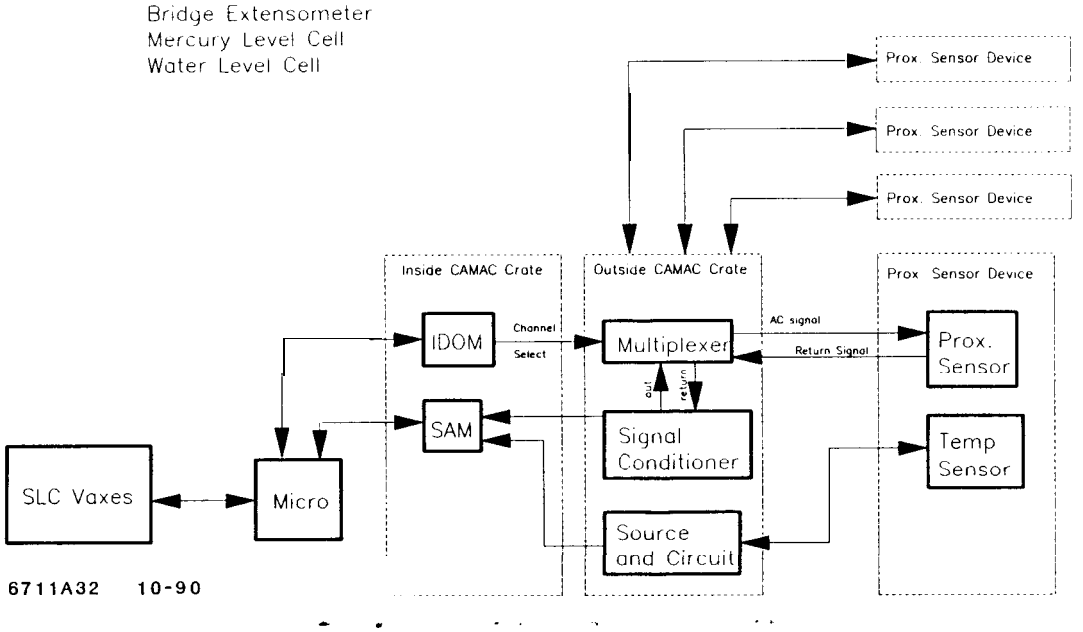

(2) Tilt Measurement Device (Control System Schematic)

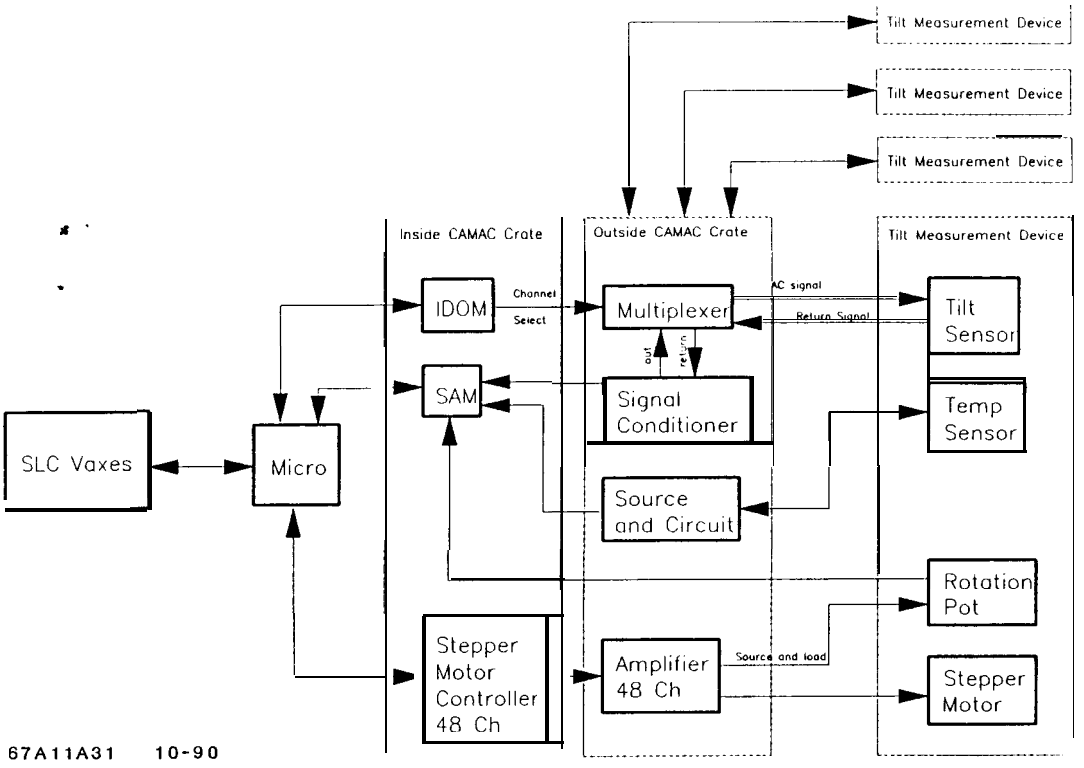

Figure 12. Schematics for the Integration of various alignment components into the overall control system, (a), (b).

(4) Wire Position Monitor (Control System Schematic)

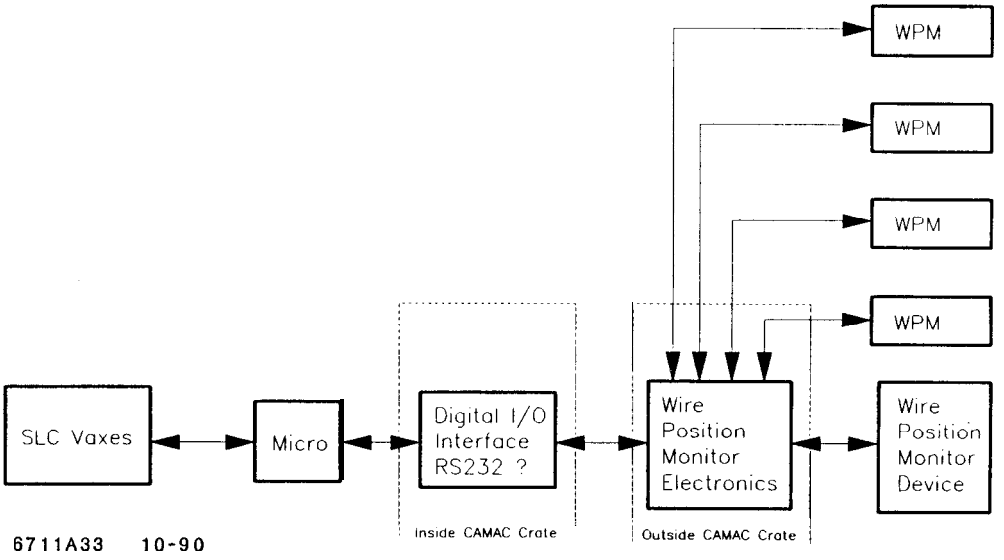

(1) Laser Alignment (Control System Schematic)

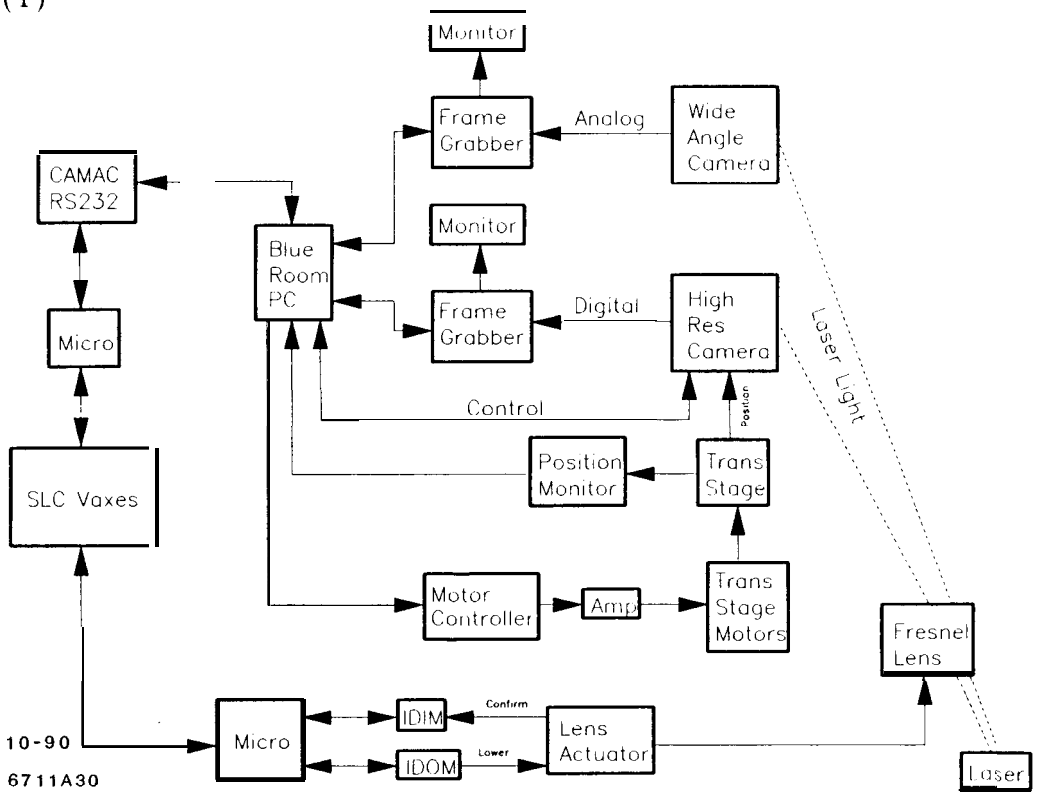

Figure 12. Schematics for the Integration of various alignment components into the overall control system, (c), (d).

6. THE HIGH-PRECISION, CAM-ACTUATED, KINEMATIC MOUNT, MAGNET-MOVER DESIGN ADOPTED

All magnetic lenses will be equipped with *magnet movers* to mechanically translate them back into line when their position has drifted by unacceptable amounts. (It remains to define the magnitude of correction at which electrical correction by means of backleg windings on the quadrupoles will perform the very small motions. We estimate this at less than 2 to 10 microns.) It is important that mechanical translations can be carried out on-line; that is, while the beam is in operation. While it is relatively easy to move objects as heavy as magnets horizontally on precision slides, vertical motion is harder to achieve.

An elegant system of *cam actuators* has been developed to position the final lenses of the SLC final focus.[18] A sketch of the original device, providing two translations and three rotations of a rigid body is shown in Figure 13. A new design, suitable for most FFTB components, but having only three degrees of freedom x, y, θ_z, has been completed. It is shown in Figure 14. Interesting features include a harmonic drive for the gear reducer box and precision ($< 1\mu$) LVDT based coordinate readout. Coarse adjustment of its base is provided for at the ±5 mm level. We assume that the final triplet assembly and the four quad-sextupole-quad packages will be mounted on the five-degree-of-freedom type mover. Our collaborators from KEK are in the process of engineering the final focus magnet mounts.

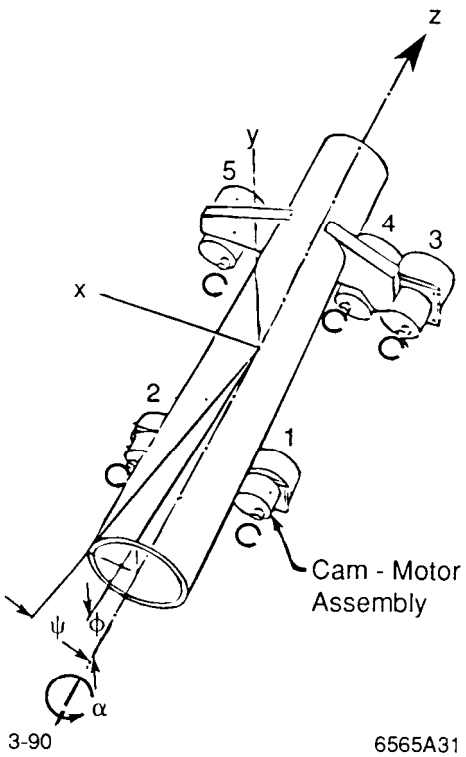

Figure 13. Sketch of a cam-operated actuator controlling five degrees of freedom.

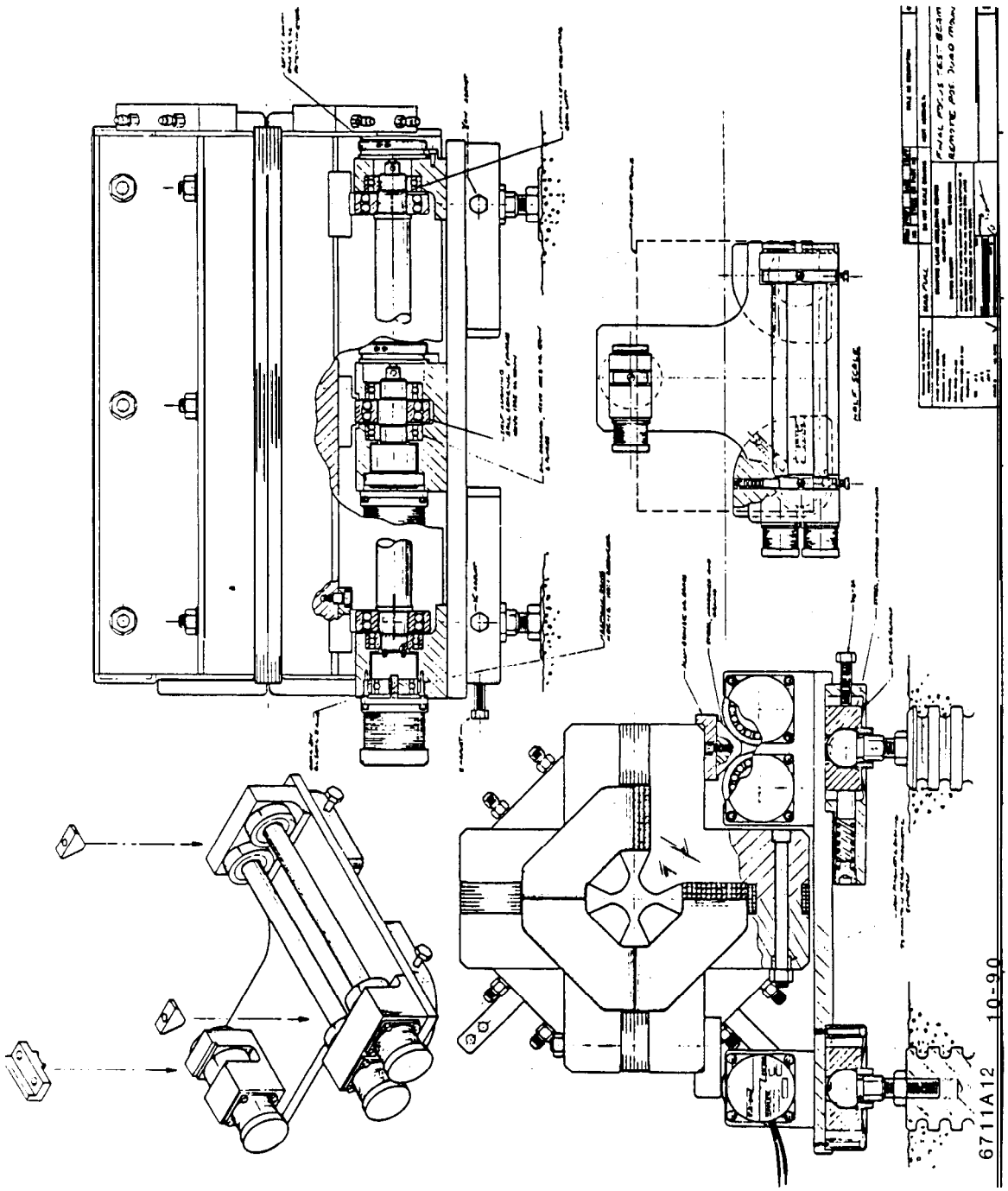

Figure 14. Design for a three-degrees-of-freedom, cam-actuated magnet mover.

7. UPDATE ON THE MAGNET FIDUCIALIZATION PROJECT

7.1. GENERAL

The magnet fiducialization proposal has been funded and expanded to include calibration and centering of Beam Position Monitors (BPMs).[19] An entirely new experimental arrangement suitable for FFTB magnet production work is being constructed and is shown in Figure 15. The table is seismically isolated from the floor and positioning stages, capable of 0.1 micron resolution in x and y, support the wire at each end. At the time of this writing, the system has just been assembled. The first magnet data is shown in Figure 16. It appears the device is living up to its promise of micron resolution and repeatability. Systematics are under investigation. BPM data is not yet available.

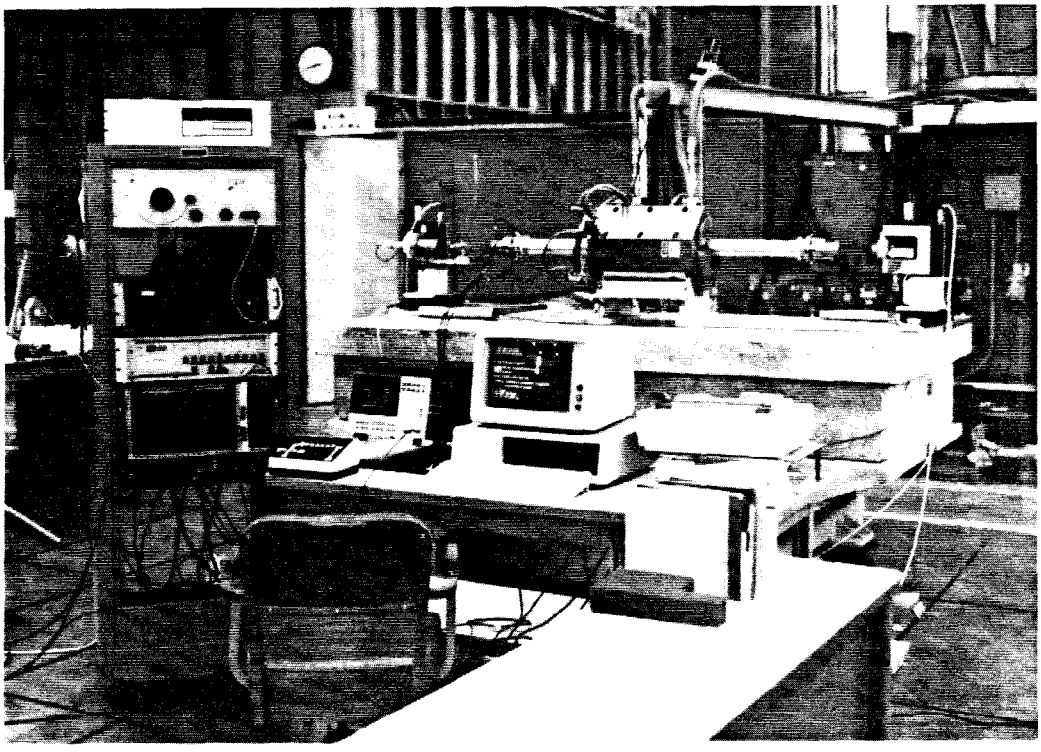

10-90 6711A13

Figure 15. New setup for magnet and beam-position monitor fiducialization.

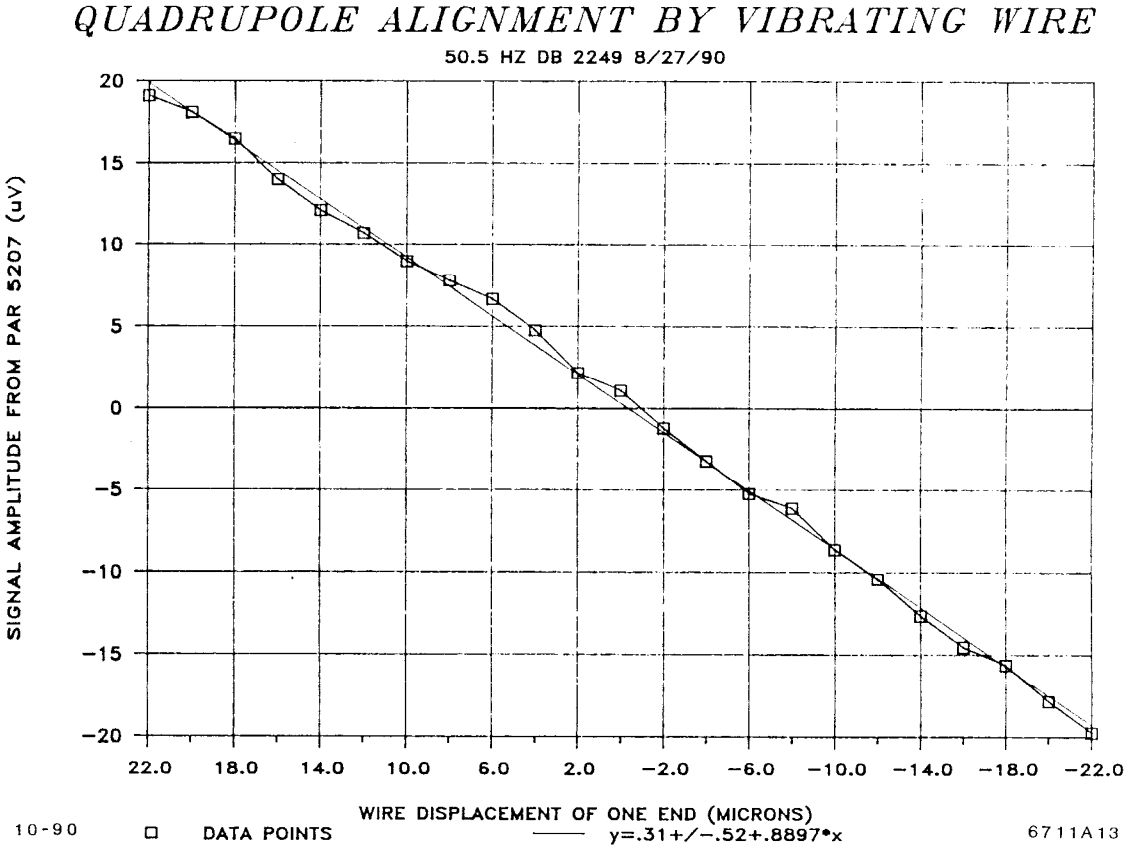

Figure 16. Lockin-amplifier output as the wire passes through the magnetic center of an FFTB-type quadrupole (motion of one end only).

7.2. DESCRIPTION

A method of magnet fiducialization, capable of micron resolution, has been described.[20] This method makes use of a single wire strung through the aperture of the quadrupole near its geometric axis. The wire is light and is tensioned by a weight at one end, so that its lowest mechanical resonant frequency is around 50 Hz. Shaken in either the vertical or horizontal plane, the voltage induced in a loop containing the wire is observed, and minimized by moving its ends by means of precision mechanical stages (see Figure 17). At minimum first-harmonic output, the wire must be along a family of lines, all of whom intersect at the nodal point of the magnet. The relative coordinates of wire position with respect to the vacuum flange, which is used as the permanently fixed mechanical reference, are obtained by a precision ring gauge. A generic design of this very simple device is shown in Figure 18. The ring of the gauge bears on the fiducial flange by three pads (two fixed, one spring loaded) so that it can be rotated in a plane perpendicular to the quad axis. The micrometer is run in so that the vibrating wire barely touches it. This condition is noted when the wire shorts to ground. The micrometer reading

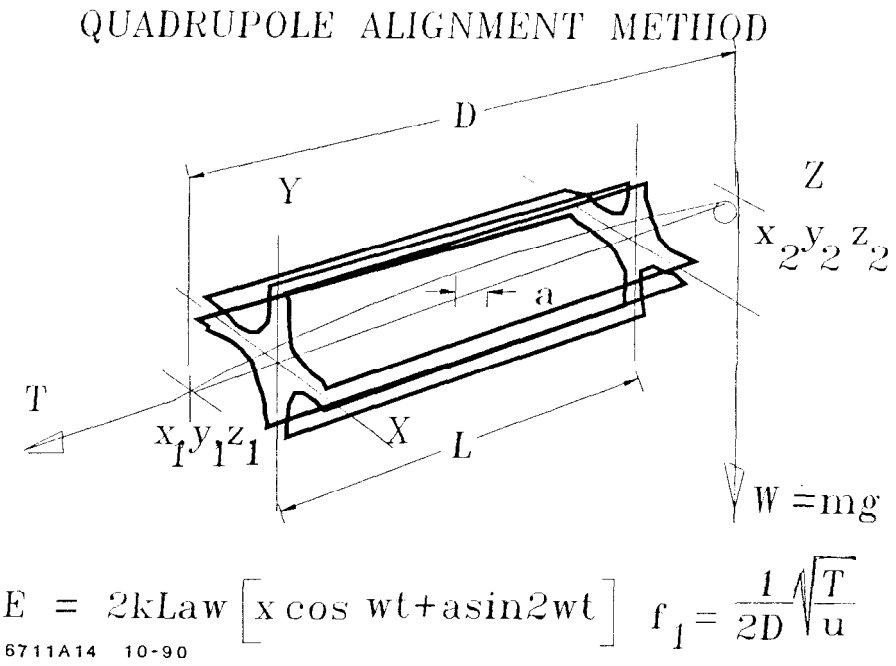

Figure 17. Principle of the singing-wire technique of locating a magnet center.

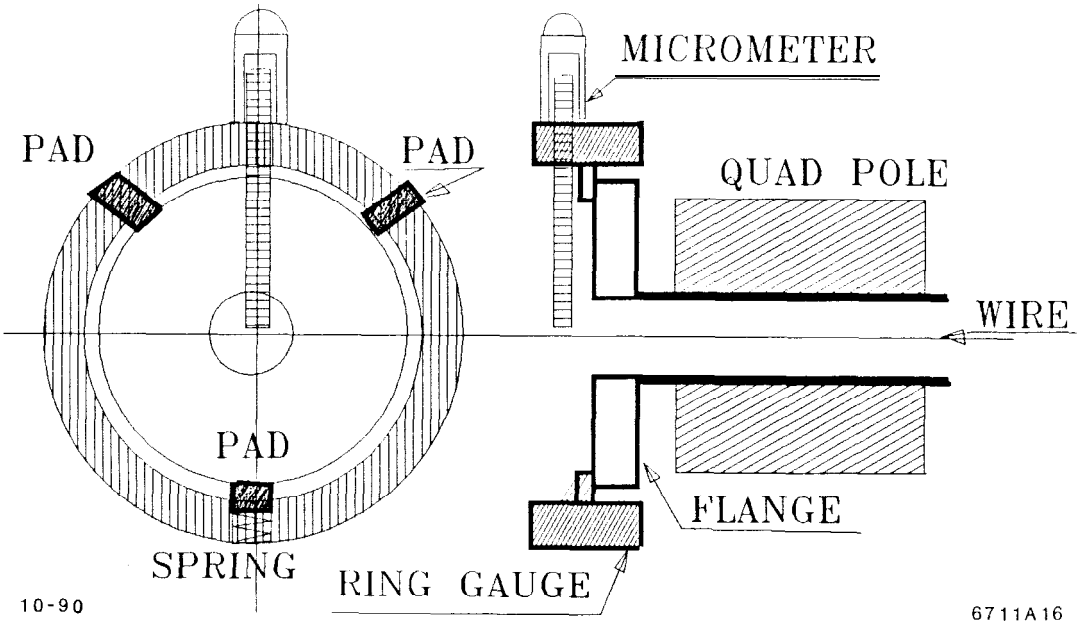

Figure 18. Sketch of a conceivable ring gauge that transfers the coordinates of the singing wire to the fiducial flange.

is recorded. The ring gauge is now rotated by 180º, and the process repeated. The wire must have been halfway between the reading with respect to the edges of the flange. The vibration process is repeated in the other coordinate, then the coordinates of the flange are transferred to the fixtures on the *tooling table* by methods described in Section 7.7.

We noticed that the setup[21] originally used to find the electrical center of the so-called *long* BPMs used in the SLC Final Focus is very similar. Let us suppose that the FFTB BPMs are internal to the vacuum chamber of the FFTB quadrupoles. They need not be of the design shown on the drawing, however good that design may have been. The essential requirement is that the vacuum housing, with its reference flange, be permanently part of the magnet assembly. The combined setup has all the requisites to measure the magnetic center and the BPM center more or less simultaneously. A fast pulse is sent down the wire and its position is sensed by the very same electronics that will be used to measure beam position in the FFTB. There are several notable consequences of this arrangement. however.

7.3. Separation of BPM Strip Center From Electronic Readout Asmmetries

The classical method of determining position from a four-strip BPM is to calculate the quantity

$$\Delta x, y = K \times \frac{(A + B) - (C + D)}{(A + B + C + D)}$$

in which A, B, C, D are the processed voltages from the four strips. Since in a linear collider in which each pulse has characteristics of its own, these voltages have to be measured simultaneously. The possibility exists, therefore, of introducing centering errors-not only from the positions of the strips and feedthroughs themselves, but from asymmetries in cable attenuations, and gain variations in the various amplifiers and ADCs as well. To separate these effects, the signals from the various electrodes will be switched in such a way as to sample each signal will all combinations of readout, solving the coupled (linear) equations that result.

7.4. BPM nodal point

We have always assumed, in the past, that a BPM has a. nodal point, for similar reasons that a quadrupole has a nodal point. We have often assumed that the BPM nodal point is halfway along the length of the strips. The centering method we propose to use will permit us to check and measure this assumption for the first time.

7.5. Sagitta of the wire and related effects.

The wire will sag under the force of gravity. Just exactly how it behaves dynamically is beyond the scope of this note. To give some orders of magnitude, we will approximate the catenary with the parabola:

$$\Delta Y = \rho X^2 / 8W$$

in which ρ is the weight/unit length of the wire, X is the distance from the center of the span, and W is the weight providing the tension. For the Z-meter-long wire of the new setup with 100 gram weight, the sag over the total length of the wire is about 30 μm. Since the position of the wire is measured at the vacuum chamber fiducial flange, what counts is the length of position monitor; for example, the length of the magnet. Since the FFTB magnets are generally 50 cm long, the sag through the magnet is about 6 μm, and must be corrected for if the vacuum flanges are used for reference outside the magnet. If, on the other hand, we are more interested in the relative offset of the magnet with respect to the BPM and the BPM is the same length, the sagitta correction falls away. In other words, we are very precisely registering the two effective centers with respect to each other.

It is our intention to prealign the quadrupole-sextupole-quadrupole packages in the laboratory. The new bed is just long enough to accomplish this aim.

7.6. Magnet and BPM Calibration

Since we have opted to provide precise (and computer read) transverse wire positioning stages, we can not only measure effective centers, but *calibrate* (i.e., measure the sensitivity as a function of offset) the BPM with similar electronics that will be used in the field. Once we have said that, it follows immediately that classical single-wire magnetic-field-strength measurements can be carried out with the same wire. A complete characterization of the quad-BPM-fiducial-flange package results. Naturally, since this calibration is performed after the last assembly operation, it must be carried out in a clean and controllable environment.

7.7. Calibration of Tooling table coordinates

The effective axes of each magnet and BPM were transferred to their fiducial flanges at each end of the magnet by the so-called ring-gauge. Since the flange is not a very convenient operational reference, it is supplemented by the *tooling table*. The ensuing package is measured in all three coordinates by a precision Coordinate Measuring Machine (CMM).[22] This machine is, of course, also used to transfer the laser target locations to their outside tooling posts. If the absolute location of the wire position monitors (WPMs) is desired, they can be calibrated by a ring gauge and incorporated into the coordinate system.

8. ACKNOWLEDGEMENTS

It is a pleasure to acknowledge the contributions made by many members of the collaboration and SLAC staff. In particular, we wish to thank those who permitted us to quote from their unpublished work in progress.

9. APPENDIX: SOME RECENT MEASUREMENTS ON THE RESEARCH YARD SITE

In contrast to the heretofore mentioned stability of the C line under the mountain of shielding that covers the BSY, the research yard is in the open and subject to the effects of the weather.

9.1. PIER THERMAL MOTION

Pier to End Station A: An experiment to determine the thermal stability of the research yard base, carried out in the Summer of 1989 (Ref. 6), concluded that portions of the concrete pad moved with respect to the base of End Station A, by as much as 0.6 mm on a daily basis, as a result of pad heating by the sun. It was therefore recommended that concrete piers be sunk into the bedrock, which were to be suitably decoupled from the surface of the concrete pad and therefore immune to surface temperature effects.

Three piers, each 3ft in diameter and 11ft deep, were subsequently poured in November 1989. They were designed to simulate the supports of the final focus test beam final quads. Measurements on their lateral position (i.e., w.r.t. End Station A) were begun March 24, following a four-month waiting period-long enough after pouring to ensure that the concrete had fully cured.

In contrast to the earlier experiment in which a Kern Mekometer was used at the limits of its stability, changes in length of the 33 meter distance were now measured, using a Hewlett-Packard interferometer. As before, the flight path was evacuated by means of a 4-inch-diameter tube to make the readings insensitive to changes in atmospheric temperature and pressure. The piers in the yard were shielded from the sun by a large tin roof, its sides loosely covered with a tarpaulin. The wind could blow through the structure freely.

Figure 19 shows results of the first data set. The data is smooth (in comparison to that taken with the Mekometer), but shows almost as much motion as the previous experiment. Although the figure shows a complete daily cycle, it is stitched together from three separate days, because the interferometer would on occasion loose count when something caused the laser beam to become misaligned. The total amplitude of motion is 300 microns (as opposed to 600 in Summer 1989); however, the temperature swings in March were not as extreme as last July.

A series of experiments were conducted next to ascertain whether the results were real or instrumental. Even though both mekometer and interferometer results are very similar, one might suspect that the interferometer head is sensitive to temperature changes. For this reason, the apparatus was moved further away from the door sill of, and into, ESA by extending the vacuum pipe another 15 feet. The fixed retroreflector on the pier (insulated against temperature changes) n-as replaced by one mounted on a servocontrolled frame, which could track minute changes in laser direction so that the instrument would not loose count for days at a time. The tilt of the door sill was monitored with a resolution of a milligon. The results are displayed in Figures 20. They are not easy to interpret.

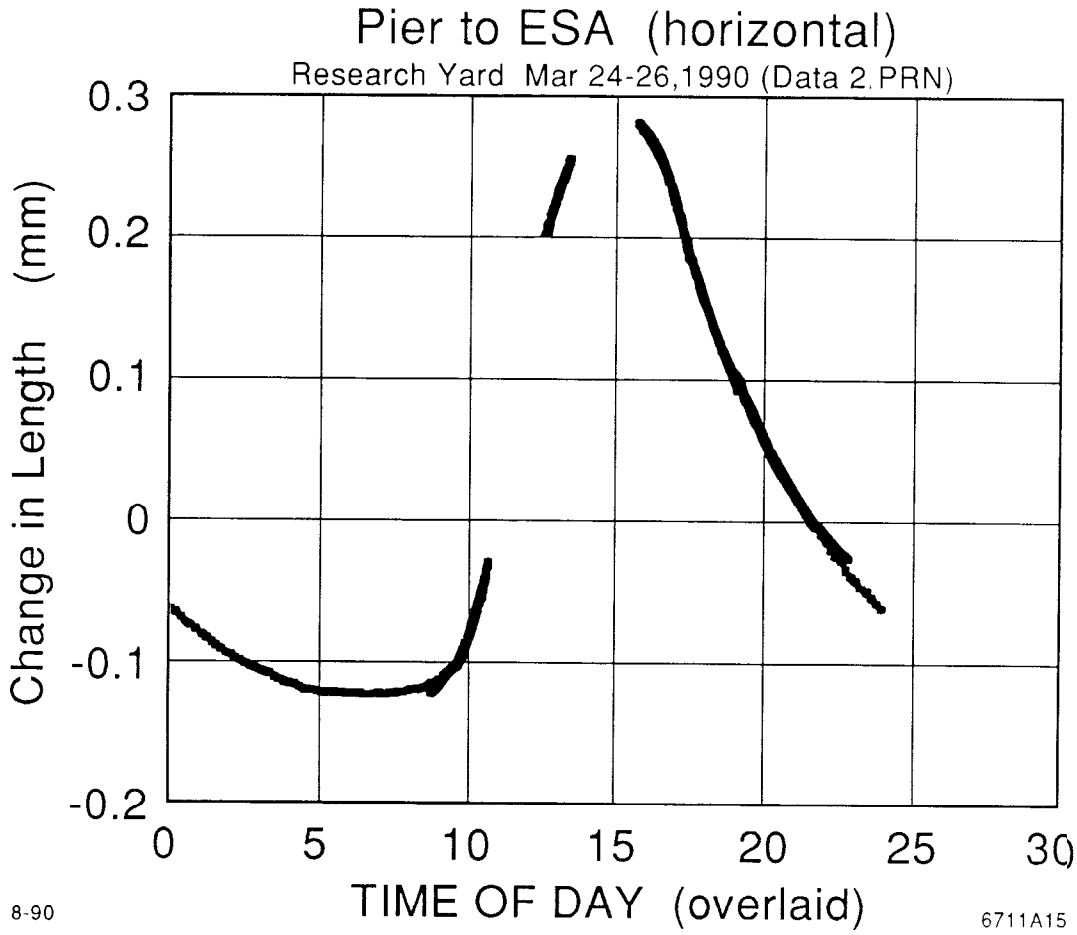

Figure 19. Change in the 33-meter distance between End Station A (ESA) and Pier A as a function of time of day.

As before, the motion lags the temperature of the concrete by about three hours when the temperature rises. However, just prior to the rise, the motion is reversed as if the floor of ESA suffers a histeretic excitation. The data clearly shows that when the sky is overcast and lesser concrete heating occurs, the motion can be as low as 50 microns. This last observation leads to the thought that, should the observed motion of the pier w.r.t. ESA also exist relative to the extension of the central beam line, one could imagine stringing a tent between the roofs of ESA and ESB to keep the sun off.

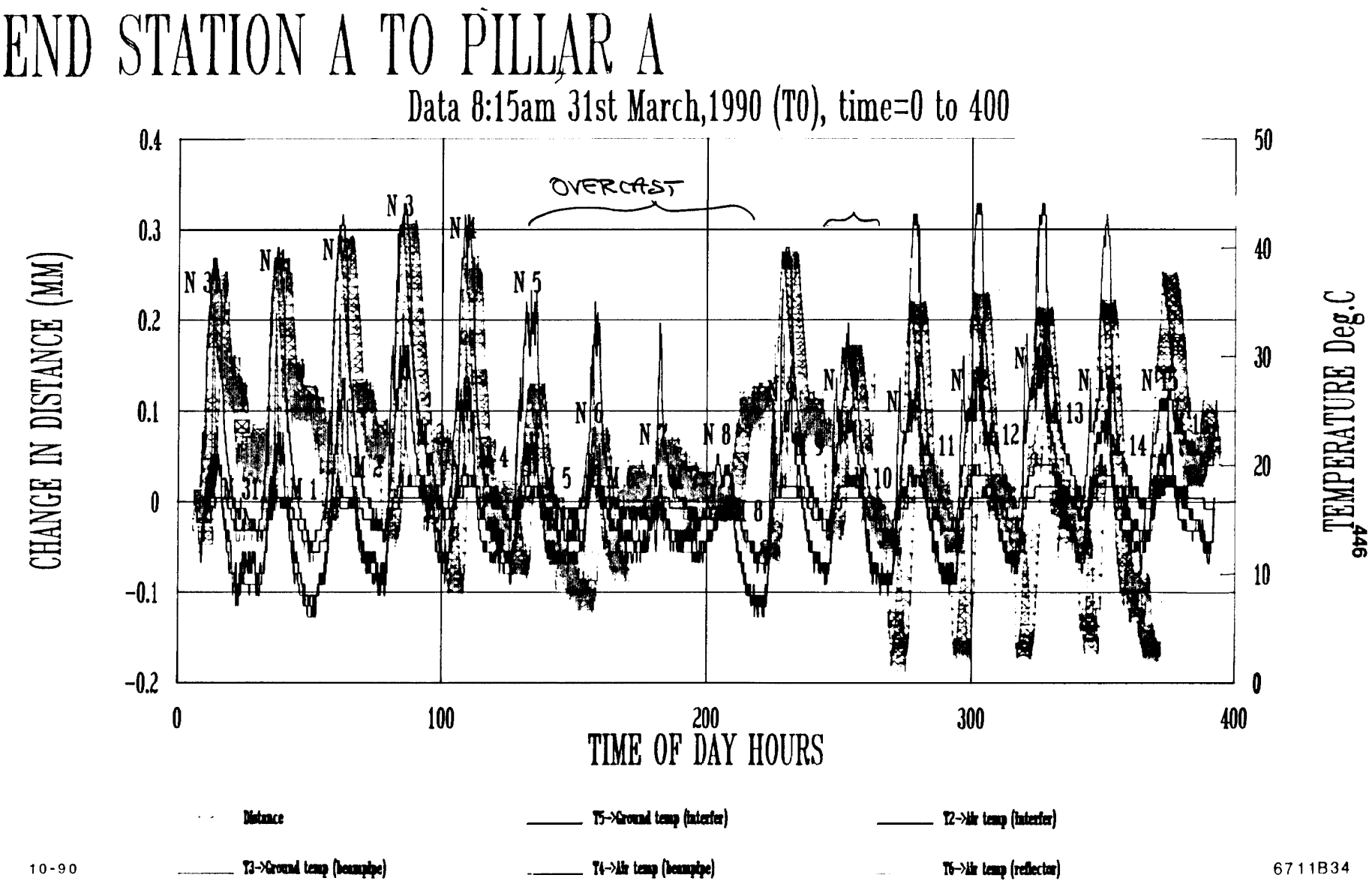

Figure 20. Three-week data of variation in the 35-meter distance from End Station A to the Final Focus Test Beam Pier

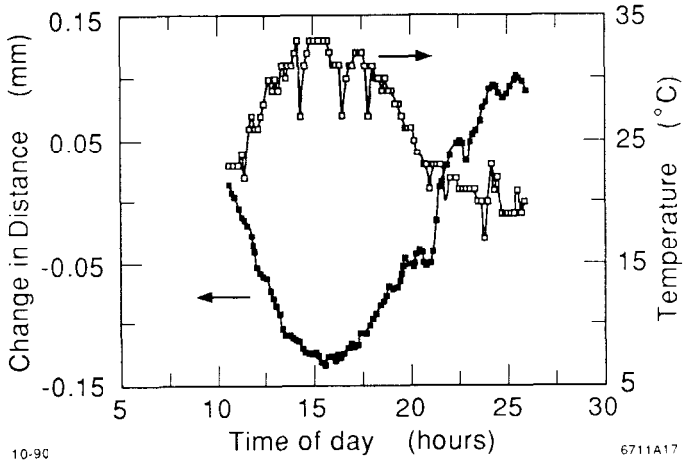

Figure 21. Variation in the distance from End Station B to Pier A.

The notion that the evacuated pipe had a leak (in both experiments) and that temperature changes of the residual gas were responsible for the observations was checked by shielding the pipe from the sun. The results were unaffected by the shielding. Changes in temperature of the port windows also cannot explain the observation. At that moment we did not know what moved, the pier or the end-station *but it became clear that our simple notion of decoupling the two by pouring a pier into the miocene bedrock was not yet a satisfactory answer.*

Pier to End Station B: The next experiment in this series was to measure variations in the distance between the piers and End Station B. The walls of the building face in the opposite direction to the sun from those of End Station A. The results are shown in Figure 21. As the temperature climbs with the rising sun the distance between ESB and the pier becomes smaller; one notes that the distance to ESA gets larger by a similar amount. This fact leads one to the interpretation depicted in Figure 22. The changing azimuth of the sun causes differential heating of the surface, and some small fraction of the resulting motion is transmitted to distort the miocene below.

Proposed* solution *to this problem: One way to keep the sun from heating the research yard surface is to string a large tent between the structures. This solution is not deemed to be very practical (high winds, etc.) and only ameliorates, but does not solve the problem. The solution of more effective decoupling between the heated concrete and the mioccne base is being investigated. Deep cuts through the concrete and into the miocene, on the edges of the FFTB housing, should act as expansion joints.

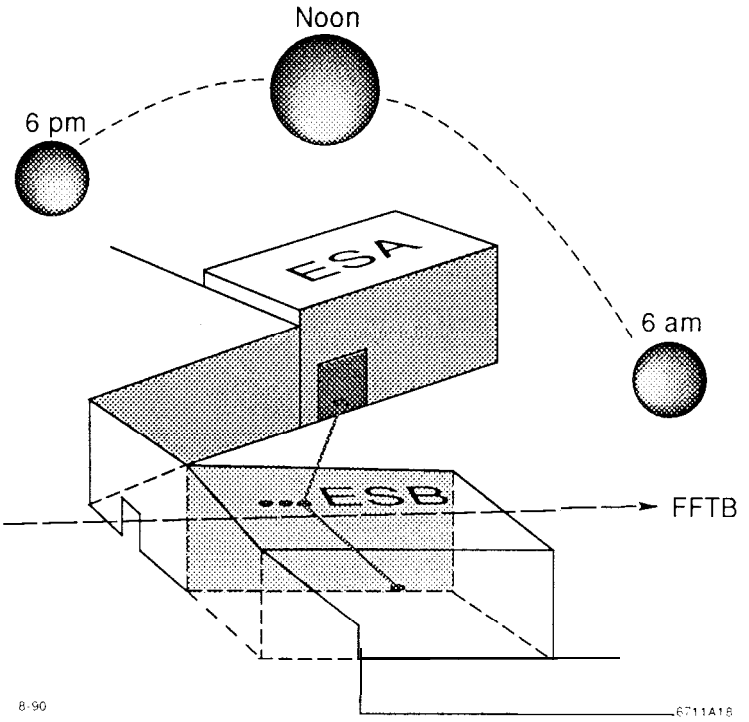

Figure 22. Differential heating of the research yard pad as a function of various azimuths of the sun during the day.

9.2. RECENT MEASUREMENTS OF VIBRATION LEVELS ON CENTRAL BEAM PIERS

In order to ascertain whether or not an active vibration isolation system[23] would be required for use in stabilizing the last lenses of the FFTB, a series of vibration level measurements were carried out together with representatives from KEK.[24]

Vertical and horizontal velocity transducers were placed on the outer piers. A typical vertical velocity spectrum is shown in Figure 23. The most prominent peak occurs at 29.875 Hz. This frequency is known to be related to LCW cooling water pumps. The minor peaks at 11.6, 12.25 and 13 are believed to be associated with machinery in the nearby cryogenics facility. With a sensitivity of 1 cm/set $\Longleftrightarrow$ 1 volt, the 55 microvolt rms signal translates to an rms coherent amplitude of 0.003 microns. The lower frequency peaks contribute comparable amounts.

The rest of the spectrum is barely above the noise of the analyser. These measurements must be repeated when the new rapid cycling injector synchrotron for SSRL operations of the SPEAR storage ring becomes operational.

Figure 24 depicts a real-time trace of a time-integrated signal proportional to real-time amplitude. With an integrator gain and time constant. yielding 0.8 microns/volt calibration we see peak-to-peak east-west amplitudes up to 0.5 volts; i.e., 0.4 microns. The period of these oscillations is very long (about 3 seconds)

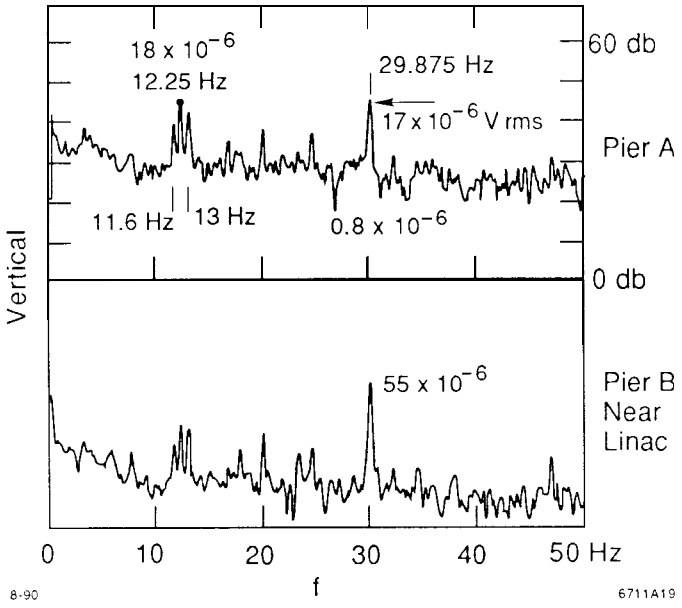

Figure 23. Spectrum of vertical ground motion velocity on Piers A and B of the research yard, taken on May 9, 1990 at 9:30 am.

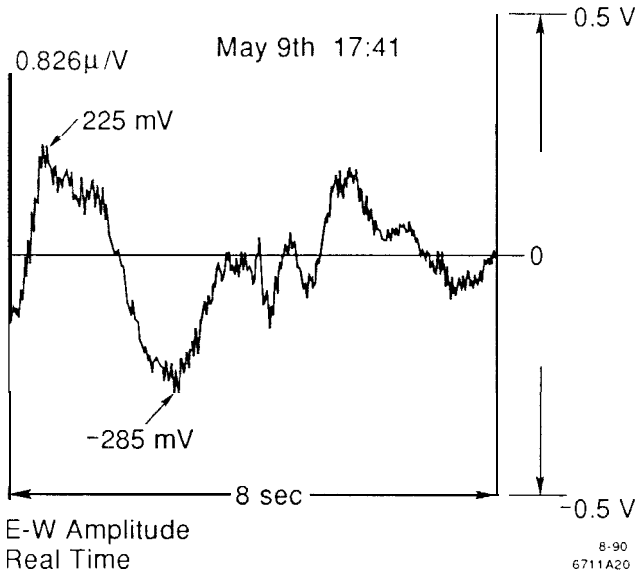

Figure 24. Real-time trace of east-west horizontal amplitude.

and therefore not considered particularly dangerous. (For discussion, see below.) Note: The roof and wall of the shed covering the apparatus was subjected to a fair amount of wind while this measurement was made. Figure 25 depicts the Probability Density Function of this real-time horizontal motion to be equivalent to about 0.1 micron. By 17:55 hours, the wind had died down and the east-west

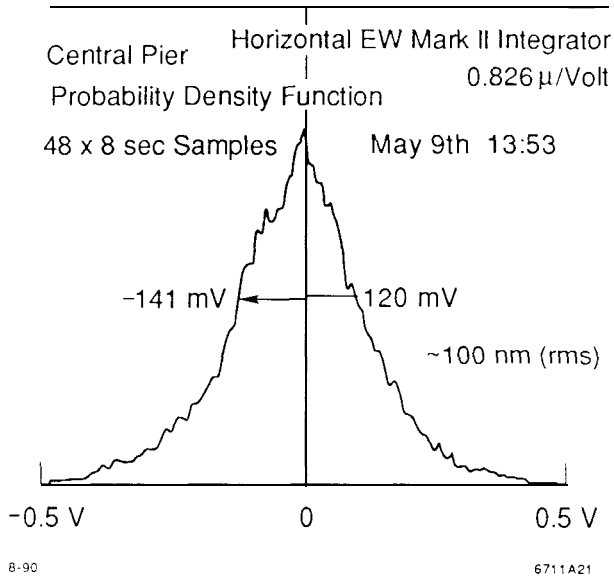

Figure 25. Probability density function of horizontal motion (windy).

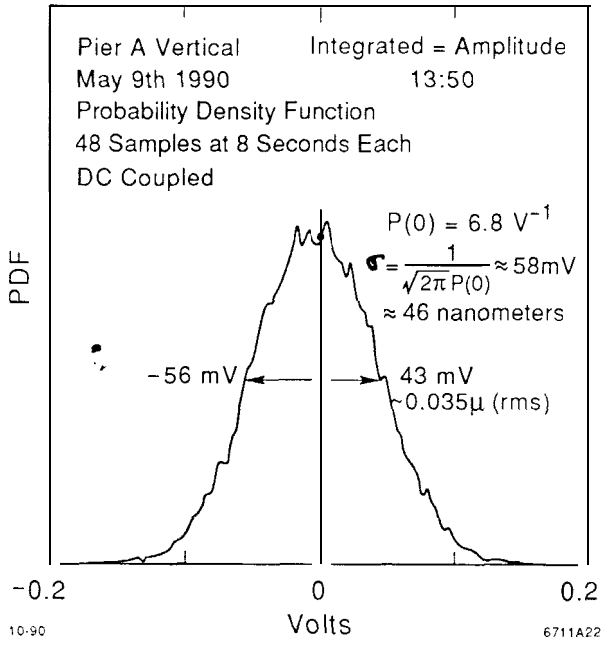

Figure 26. Probability density function of vertical amplitude on Pier A.

motion had fallen a factor of two. The vertical motion (see Figure 26) remained equivalent to about 0.05 microns rms.

A measurement of the shear-wave velocity in the bedrock is afforded by drop ping a lead brick and measuring the time-of-arrival at vertical sensors mounted on the outer piers as shown in Figure 27. The distance between the piers is 5.5 meters

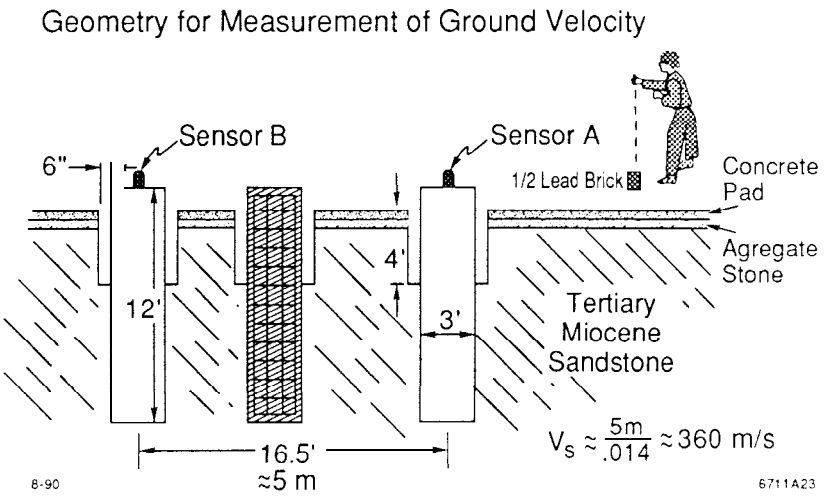

Figure 27. Geometry of the piers used to make ground velocity measurement.

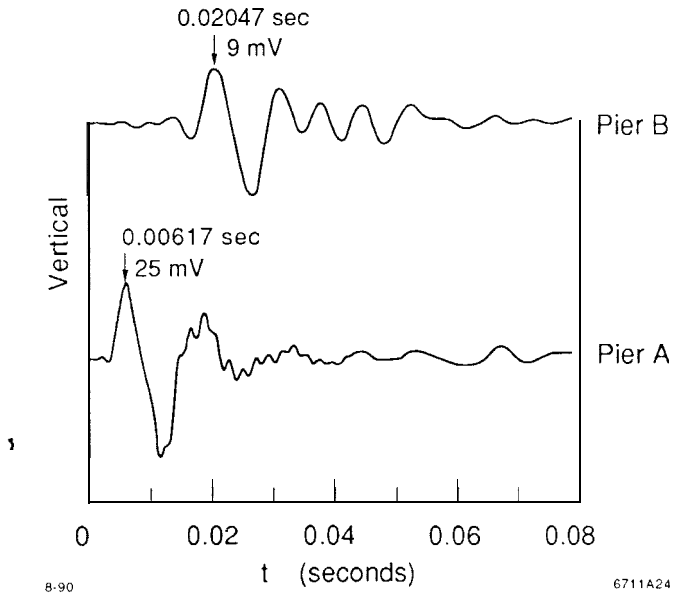

Figure 28. Display of time-of-arrival of sound on Piers A and C.

and the arrival time difference which can be read from Figure 28 is 14 milliseconds, yielding a not unreasonable shear-wave velocity for this material at this depth. of about 400 meters/second. Since all disturbances with wavelengths greater than, say, 75 interpier distances will be 92% coherent (sin $2\pi/75 \approx .08$) frequencies below one Hertz will not be dangerous to this extent. However, larger distances require the absence of disturbances above still lower frequencies. Generally speaking, the larger amplitudes (up to one micron) due to ocean wave activity on the Pacific rim occur only during heavy winter storms at sea and have periods in the many seconds.

REFERENCES

[1]The following laboratories are currently contributors: KEK, Japan; Novosibirsk, USSR; Orsay, France; DESY, Germany.

[2]Values of the invariant emittances used in this design are $\gamma\epsilon_y$ = 3 x 10^{-6} and $\gamma\epsilon_x$ = 3 x 10^{-5} radian-meters. Such values are believed to be consistent with uncoupled SLC values.

[3]"Final Focus Test Beam Alignment-A Draft Proposal" G. E. Fischer, R. E. Ruland, SLAC-TN-89-02 (1989).

[4]K. Oide, "Design Optics for the Final Focus Test Beam at SLAC," Proc. of the 1989 IEEE Particle Accelerator Conf., 1989, p. 1319.

[5]We benefitted from conversations with Dr. G. A. Voss, DESY, about this point and his suggestion to monitor quadrupole positions continuously by the use of *stretched wires.*

[6]Some comments regarding the site of the Final Focus Test Beam, G. Fischer et al., 1989, unpublished.

[7]The tolerances listed in this section were derived by John Irwin and Ghilain Roy, Spring 1990, unpublished.

[8]For example, the ME500 made by Kern, Switzerland.

[9]See Ref. 3.

[10]For example, Chesapeake Laser Systems, Inc., 4473 Forbes Blvd., Lanham, MD 20706.

[11]The mechanical and electrical development of the wires is being carried out by Drs. F. Loeffler, W. Schwarz, and F. Peters, DESY.

[12]Some more recent applications may be found in "Alignment and Vibration Issues in TeV Linear Collider Design," G. E. Fischer, Part. Accel. 31, 47-55 (1990).

[13]W. Schwarz, "Wire Measurements for the Transversal Control of the FFTB-Magnets," Paper D4, these proceedings.

[14]See Ref. 3 or Proc. of the 1st Int. Workshop on Accelerator Alignment, SLAC, 1990.

[15]Model HPT-375G-A-12-100-B-D, Capacitec, P.O. Box 819, 87 Fitchburg Rd., Ayer, Mass 01432, (505) 772-6033, with series 4000 signal processing.

[16]Kaman Instrumentation Corp., 1500 Garden of the Gods Rd., P.O. Box 7463, Colorado Springs, Co 80933, Model KD-5100 Series, used to steer telescope mirrors in the microradian range.

[17]These concepts were provided by V. Bressler.

[18]G. Bowden, G. Putallaz, "A Positioning Mechanism for the Final Quadrupole Triplet," Final Focus Memo dated 3/10/85.

[19]This project is being coordinated by Dr. S. Williams.

[20]G. Fischer, J. Cobb, and D. Jensen, SLAC-TN-89-01 (1989).

[21]Gordon Bowden et al., DWG No. SA 235-417-01-R2, originally dated 11-11-85.

[22]For example, in the SLAC laboratory, the Leitz Model PMM 12106 Enhanced Accuracy CMM, Wetzlar, Germany.

[23]See for example, N. Ishihara et el., Part. Accel. 31, 57-62 (1990).

[24]K. Oide, H. Nakayama, and N. Yamamoto took part in the measurements May 9, 1990.